EVALUATION OF FUNCTIONAL CHANGES IN AKR OVEREXPRESSING COLORECTAL CELL LINE SW480

A THESIS SUBMITTED TO
THE GRADUATE SCHOOL OF NATURAL AND APPLIED SCIENCES
OF
MIDDLE EAST TECHNICAL UNIVERSITY

BY

ÇAĞDAŞ ERMİŞ

IN PARTIAL FULFILLMENT OF THE REQUIREMENTS
FOR
THE DEGREE OF MASTER OF SCIENCE
IN
BIOCHEMISTRY

FEBRUARY 2021

Approval of the thesis:

EVALUATION OF FUNCTIONAL CHANGES IN AKR OVEREXPRESSING COLORECTAL CELL LINE SW480

submitted by **ÇAĞDAŞ ERMİŞ** in partial fulfillment of the requirements for the degree of **Master of Science** i**n Biochemistry, Middle East Technical University** by,

Prof. Dr. Halil Kalıpçılar
Dean, Graduate School of **Natural and Applied Sciences** _____

Assoc. Prof. Dr. Yeşim Soyer
Head of the Department, **Biochemistry** _____

Prof. Dr. Sreeparna Banerjee
Supervisor, **Biology, METU** _____

Assoc. Prof. Dr. İrem Erel Göktepe
Co-Supervisor, **Chemistry, METU** _____

Examining Committee Members:

Prof. Dr. Nülüfer Tülün Güray
Biology, METU _____

Prof. Dr. Sreeparna Banerjee
Biology, METU _____

Assoc. Prof. Dr. İrem Erel Göktepe
Chemistry, METU _____

Assoc. Prof. Dr. Erkan Kiriş
Biology, METU _____

Assist. Prof. Dr. Onur Çizmecioğlu
Molecular Biology and Genetics, Bilkent Uni. _____

Date: 02.02.2021

I hereby declare that all information in this document has been obtained and presented in accordance with academic rules and ethical conduct. I also declare that, as required by these rules and conduct, I have fully cited and referenced all material and results that are not original to this work.

Name Last name : Ermiş, Çağdaş

Signature :

ABSTRACT

EVALUATION OF FUNCTIONAL CHANGES IN AKR OVEREXPRESSING COLORECTAL CELL LINE SW480

Ermiş, Çağdaş
Master of Science, Biochemistry
Supervisor : Prof. Dr. Sreeparna Banerjee
Co-Supervisor: Assoc. Prof. Dr. Irem Erel Göktepe

February 2021, 78 pages

The Aldo-Keto Reductases (AKR) are nicotinamide adenine dinucleotide (NAD(P)H) dependent oxidoreductases that function in phase 1 metabolism by reducing aldehydes and ketones into primary and secondary alcohols. In this protein superfamily, the expression of AKR1B1 and AKR1B10 enzymes have been linked by us and others to colorectal cancer (CRC). Over-activation of these enzymes in the presence of excess glucose can result in the activation of the polyol pathway, which causes oxidative stress and might contribute to the progression of cancer. Substrates of the AKR enzymes vary from sugars to various chemical carcinogens. Many studies suggest that chemotherapy drugs can also be metabolized by these enzymes, leading to drug resistance. On the other hand, a link between these enzymes and a mesenchymal phenotype has also been gaining attention.

In this study, we aimed to investigate the effects of overexpression of two AKR enzymes, AKR1B1 and AKR1B10, on CRC cell line SW480, which does not have the endogenous expression of either gene. We observed that AKR1B1

overexpressing cells showed higher motility and weaker cell-cell adhesion but no significant change in proliferation. These data are consistent with previous findings on a strong and significant positive correlation between the expression of AKR1B1 and several different mesenchymal markers. We also show for the first time that serum-starved AKR1B1 expressing cells expressed higher protein levels of a rate-limiting enzyme of the pentose phosphate pathway, most likely as a means to cope with the increased oxidative stress in the starved cells. AKR1B10 overexpressing cells were significantly less motile, showed a slower cell cycle progression and a reduced clonogenic potential. Overall, our data corroborate previous reports on the highly divergent effects of two very closely related enzymes in colorectal cancer.

Keywords: Colorectal Cancer, AKR1B1, AKR1B10, SW480

ÖZ

AKR AŞIRI İFADELENEN KOLOREKTAL HÜCRE HATTI SW480'DEKİ FONKSİYONEL DEĞİŞİKLİKLERİN DEĞERLENDİRİLMESİ

Ermiş, Çağdaş
Yüksek Lisans, Biyokimya
Tez Yöneticisi: Prof. Dr. Sreeparna Banerjee
Ortak Tez Yöneticisi: Doç. Dr. İrem Erel Göktepe

Şubat 2021, 78 sayfa

Aldo-Keto Redüktazlar (AKR), aldehitleri ve ketonları birincil ve ikincil alkollere indirgeyerek faz 1 metabolizmasında işlev gören nikotinamid adenin dinükleotit (NAD(P)H) bağımlı oksidoredüktazlardır. Daha önce yapılan çalışmalarla da desteklenen, bu protein süper ailesinde AKR1B1 ve AKR1B10 enzimlerinin ekspresyonu bu calışma tarafından da kolorektal kansere (CRC) bağlanmıştır. Fazla glikoz varlığında bu enzimlerin aşırı aktivasyonu, oksidatif strese neden olan ve kanserin ilerlemesine katkıda bulunabilen poliol yolağının aktivasyonuna neden olabilir. AKR enzimlerinin substratları, şekerlerden çeşitli kimyasal kanserojenlere kadar değişir. Birçok çalışma, kemoterapi ilaçlarının da bu enzimler tarafından metabolize edilebileceğini, bu durumun da ilaç direncine yol açabileceğini göstermektedir. Öte yandan, bu enzimler ile mezenkimal fenotip arasındaki bağlantı da değer arz etmektedir.

Bu çalışmada, iki AKR enziminin, AKR1B1 ve AKR1B10'un aşırı ekspresyonunun, her iki genin de endojen ekspresyonuna sahip olmayan CRC hücre hattı SW480 üzerindeki etkilerini araştırmayı amaçladık. AKR1B1'i aşırı ifade eden hücrelerin

daha yüksek motilite ve daha zayıf hücre-hücre yapışması gösterdiğini, ancak proliferasyonda önemli bir değişiklik olmadığını gözlemledik. Bu veriler, AKR1B1 ifadelenmesi ile birkaç farklı mezenkimal belirteç arasındaki güçlü ve anlamlı pozitif korelasyon hakkındaki önceki bulgularla tutarlıdır. Ayrıca ilk kez, açlığa tabi tutulmuş AKR1B1 eksprese eden hücrelerin, pentoz fosfat yolağının hız sınırlayıcı enziminden daha yüksek protein seviyelerini eksprese ettiğini, büyük olasılıkla aç hücrelerde artan oksidatif stresle başa çıkmanın bir yolu olduğunu gösterdik. AKR1B10 aşırı ifade eden hücreler önemli ölçüde daha az hareketliydi, daha yavaş bir hücre döngüsü ilerlemesi ve azalmış bir klonojenik potansiyel gösterdi. Genel olarak, verilerimiz kolorektal kanserde çok yakından ilişkili iki enzimin oldukça farklı etkileri hakkındaki önceki raporları doğrulamaktadır.

Anahtar Kelimeler: Kolorektal Kanser, AKR1B1, AKR1B10, SW480

To my family and love…

ACKNOWLEDGMENTS

The author wishes to express his deepest gratitude to his supervisor Prof. Dr. Sreeparna Banerjee, and co-supervisor Assoc. Prof. Dr. İrem Erel Göktepe for their guidance, advice, criticism, encouragements, and insight throughout the research.

The author would also like to thank Aleksandra Elbakyan for creating such a wonderful platform like Sci-hub and making science accessible for everybody from everywhere around the world.

The author would also like to thank all the jury members; Prof. Dr. Nülüfer Tülin Güray, Assoc. Prof. Dr. Erkan Kiriş and Assist. Prof. Dr. Onur Çizmecioğlu for their contributions.

The author would also be deeply grateful and thankful to the former and present Lab B59 family. Many thanks to Burak Kızıl for being such a good buddy in an out of the lab and being a wide variety of things from gym-bro to Pokemon trainer friend and gardening buddy, Melis Çolakoğlu, for teaching many techniques and being able to put a smile on the faces, Aydan Torun for sharing the love of the music and being a good companion for everything, Hazal Hüsnügil for trolling anytime and uplifting the moods, Ezgi Güleç for being sports and spheroid buddy and bringing delicious treats, Göksu Oral for keeping the chemistry spirit up high and running and Sinem Ulusan for being the partner of destiny in this path.

The author would also like to hug all AKR Team members for being such good (lab) partners in crime. Many thanks to Hoşnaz Tuğral for sharing the ‘obscene’ interest and giving a hand in every time when there is a need for help, Ismail Güderer for suffering this entire process together, teaching a considerable number of things, and being a perfect (from time-to-time) lab partner/partner in crime and finally Esin Gülce Seza for being such a wonderful PI/mother/best friend/drinking buddy/lab

partner/cell culture partner and more things that author cannot fit here throughout the entire process. Your help is priceless…

The author would also like to thank Ahmet Toraman, Ekin Doğmuş, Oğuzcan Taneroğlu, and departed Ali Baran Göğüş for being such wonderful and close friends. Without those people, the author cannot find the spirit to hold on to his ideals. Thanks for all the drinks and countless sleepless rave nights. You mean a lot to the author…

The author would also like to thank his one and only love Damla Şahin for sharing her love, passion, and kindness from the very beginning of bachelor's to the end of master's and hopefully to the end of life. Without her countless support and companionship, this thesis was impossible to finish.

And finally, the author would like to thank his entire family for giving the love and passion for science and supporting him throughout the entire process and his life. Many thanks to Menekşe Ermiş Şen, who became the best sister in the world, from playing Pokemon GO together for countless hours to doing experiments together until the dawn in this process and also giving the author the best nephew in the world.

This work is partially funded by Scientific and Technological Research Council of Turkey under grant number TUBİTAK 118Z688.

TABLE OF CONTENTS

LIST OF TABLES

TABLES

LIST OF FIGURES

FIGURES

LIST OF ABBREVIATIONS

ABBREVIATIONS

AKR Aldo-keto reductases

CRC Colorectal cancer

NAD(P)H Nicotinamide adenine dinucleotide phosphate

EMT Epithelial-Mesenchymal Transition

PBS Phosphate Buffer Saline

TBS-T Tris Buffer Saline-Tween 20

ATP Adenosine triphosphate

DAMP Damage -associated molecular pattern

ROS Reactive Oxygen Species

PPP Pentose Phosphate Pathway

EV Empty Vector

O/E Overexpression

CHAPTER 1

INTRODUCTION

1.1 Cancer Cell Metabolism

According to the National Cancer Institute, USA, cancer is defined as the uncontrolled division and spreading of cells into surrounding tissues (National Cancer Institute, 2015). Several genetic events like deletions, insertions, amplifications, and substitutions in the DNA sequence resulting from failed DNA replication machinery and other intracellular/extracellular factors transform healthy cells into cancer cells.

In their seminal paper, Hanahan and Weinberg have identified several "hallmarks of cancer" that include: maintaining proliferating signaling, avoiding growth suppressors, resisting cell death, replicative immortality enabling, angiogenesis induction, and finally invasion and metastasis activation (Figure 1). The most common characteristic of cancer cells is their ability to preserve chronic proliferation. Healthy tissues control the release and production of growth-promoting signals that regulate cell growth and division, as well as cell cycle entry and progression to maintain homeostasis. On the other hand, most of these signals are deregulated in cancer cells. Growth factors are the most common types of enabling signals that bind to cell-surface receptors containing intracellular tyrosine kinase domains. Upon binding, these receptors emit signals to a branched intracellular signaling pathway that regulates cell cycle progression, cell growth, and other biological properties such as energy metabolism and cell survival. Deregulation of these signals in cancer cells occurs in multiple ways, such as producing autocrine growth factor ligands for proliferative stimulation, sending

signals to healthy cells in order to stimulate the production of various growth factors that support the tumor-associated stroma (Bhowmick *et al*., 2004, Cheng *et al*., 2008) and deregulating receptor signaling by elevating receptor protein levels displayed at the cell surface to enhance response to growth factor ligands (Hanahan & Weinberg, 2011). In their updated hallmarks of cancer paper, Hanahan and Weinberg also identify several emerging hallmarks of cancer, which include evading immune destruction and deregulation of cellular energetics. This and a considerable body of literature published on cellular metabolism in cancer in recent years have highlighted the growing importance of the role of aberrant activation of metabolic pathways in cancer progression.

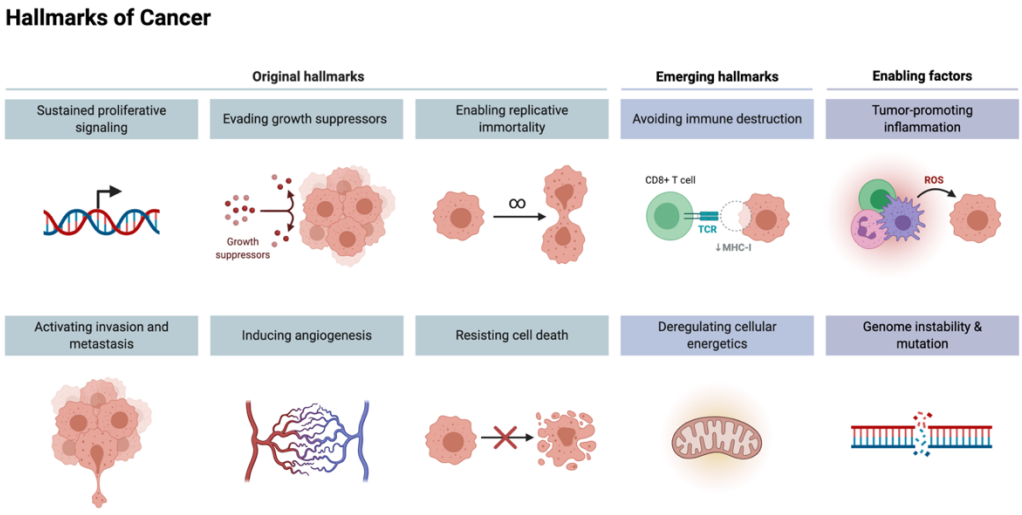

Figure 1. *The hallmarks of cancer*

Sustained proliferative signaling evades growth suppressors, enabling replicative immortality, activating invasion and metastasis, inducing angiogenesis, and resisting cell death. Emerging hallmarks include avoiding immune destruction and deregulating cellular energetics (Hanahan & Weinberg, 2011) Created with BioRender.com.

A distinct property seen in cancer cell metabolism is the "Warburg effect." Alterations in cellular metabolism push the cells to produce energy via glycolysis

and lactic acid fermentation regardless of the oxygen level (Yang & Lu, 2015). Per unit of glucose, aerobic glycolysis is an inefficient way to produce ATP compared to mitochondrial respiration [2 vs. 33.45 molecules of ATP (Mookerjee *et al*., 2017)]. However, compared to mitochondrial respiration, aerobic glycolysis produces ATP faster since the speed of lactate production from glucose is approximately 100 times faster than the complete oxidation of glucose in the mitochondria (Shestov *et al*., 2014). Nonetheless, recent studies have shown that the amount of ATP is not a limiting factor since the ATP demand never reaches the limiting values in rapidly growing tumor cells (Lunt & Vander Heiden, 2011). Warburg effect and other metabolic alterations entail cancer cells to undergo increased anabolism and biomass production. This includes nucleotide, amino acid, and lipid synthesis, altered anti-metabolic stress responses to maintain homeostasis and survival, and finally reprogramming gene expression in a metabolism-dependent way to support cell growth and rapid division (Wang *et al*., 2018).

Tumor acidosis, which results from hypoxia in the inner mass of cells due to the lack of proper perfusion, is one such metabolic event that can alter gene expression. Hypoxia induces the activity of the transcription factor HIF1α, leading to the transcriptional upregulation of its target genes such as glucose transporters and several glycolytic enzymes to convert glucose to pyruvate (Nakazawa *et al*., 2016). As by-products of this fermentation process, lactate and H^+ are generated, and when combined, they produce lactic acid, which acidifies the tumor microenvironment (Corbet & Feron, 2017). Recent studies highlight the importance of lactic acid on cancer metabolism as an effector molecule rather than just a by-product of glycolysis. Barnes *et al*. (2020) showed that in CRC cell lines, the presence of lactic acid could induce resistance to the Akt inhibitor uprosertib, an anti-cancer drug currently undergoing clinical trials. Other studies have shown that lactate might act as an agonist for the receptor GPR81 to upregulate the expression of genes linked with lactate metabolism and survival (Lee *et al*., 2016). Lactate has been shown to increase the expression of the anti-apoptotic protein Bcl-2 via the PI3K/Akt/mTOR signaling pathway, promoting survival under glucose deprivation (Huang *et al*.,

2015). In addition, a lactate dehydrogenase B mediated conversion from lactate to pyruvate has been shown to facilitate lysosomal acidification and autophagy, which is necessary for survival under nutrient stress conditions, such as glucose deprivation (Brisson *et al*., 2016). Tumor acidosis initiates an immune response by acting as a danger-associated molecular pattern (DAMP) and attracts immune cells into the tumor. This acidic microenvironment produced by cancer cells has been shown to delay neutrophil apoptosis, inhibit the cytotoxic response of CD8+ T-cells and IFN-γ production from TH1 cells (Diaz *et al*., 2018). Additionally, a hypoxic environment promotes immune cells to produce reactive oxygen species (ROS) and induce the expression of transcription factor NF-κB, which in turn can drive the regulated expression of mitogenic cytokines. Cancer cells are dependent on these cytokines for growth, and the immune cells present in the tumor are programmed to continually release these factors (Whiteside, 2008). ROS formation is a tightly regulated process since too much ROS production can lead to various cell death forms (Ray *et al*., 2012). Elevated ROS formation during acidosis and hypoxia can cause cellular stress and secretion of growth factors that can contribute to cellular proliferation (Pavlova & Thompson, 2016).

Overall, it can be concluded that cancer cells acquire the ability to alter their metabolism in a way to promote tumor growth and survival depending on intrinsic and extrinsic mechanisms such as changes in gene expression and alterations in the microenvironment around them.

1.2 Metabolic Pathways In Cancer

1.2.1 Glycolysis and Lactic Acid Production

In 1930 Warburg determined that cancer cells prefer to use glucose to produce lactic acid more than healthy tissues. Although it demonstrates adaptation to intratumoral

hypoxia, which results in angiogenesis and blood flow, glycolysis appears to occur in the existence of decent oxygen levels and is therefore termed aerobic glycolysis. In aerobic metabolism, more energy is produced than aerobic glycolysis due to the fact that glycolysis produces 2 mol ATP per glucose, yet in oxidative metabolism, 30-32 mol ATP is produced for each glucose molecule. Although glycolysis provides an insufficient amount of ATP, cancer cells prefer glycolysis for producing biomass like fatty acids, amino acids, and nucleotides for new cells. The biomass production mainly happens during the Pentose Phosphate Pathway (PPP) for nucleotide synthesis and Tricarboxylic Acid Cycle (TCA) for lipid and amino acid synthesis (Heiden *et al*., 2009).

1.2.2 Pentose Phosphate Pathway (PPP)

The phosphogluconate pathway (Pentose Phosphate Pathway, PPP) is one of the branches that utilizes glucose-6-phosphate (G-6-P. In PPP, Ribulose-5-phosphate (Ru-5-P) results from the oxidative carboxylation of G-6-P. Ribose-5-phosphate (R-5-P) is formed by isomerization of Ru-5-P, which leads to produce nucleotide and metabolize non-oxidative PPP branch to propagate fructose-6-phosphate (F-6-P) and glyceraldehyde-3-phosphate (G-3-P) by using numerous enzymatic steps (Riganti *et al*., 2012, Patra & Hay, 2014). The PPP includes the oxidative and non-oxidative steps. In oxidative PPP, Glucose-6-phosphate dehydrogenase (G6PD) catalyzes the reduction of NADP+ to NADPH while G-6-P is oxidized into 6-phosphogluconolactone (6-PG). Allosteric enzymes pursue many reversible reactions in the non-oxidative branch in order to adapt to the metabolic requirements of cells. F-6-P and G-3-P can be formed in both the non-oxidative PPP branch and the glycolysis, as stated before (Figure 2).

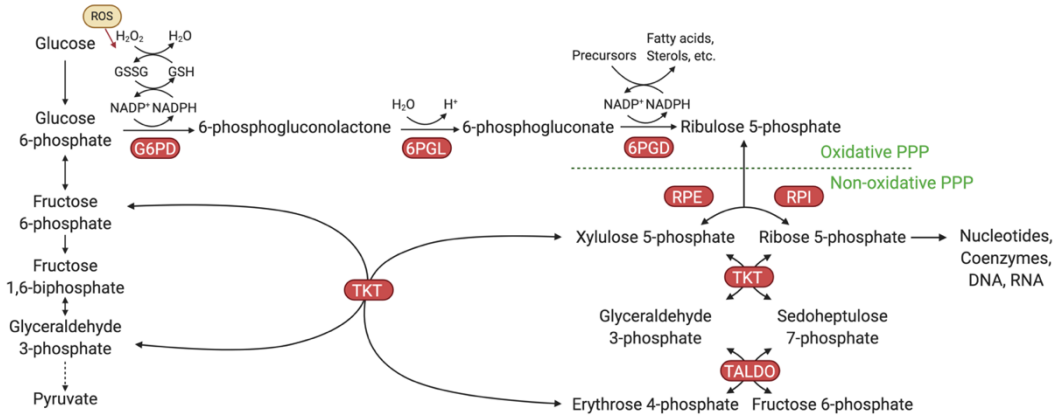

Figure 2. *Pentose phosphate pathway (PPP)*

After the first step of glycolysis, the PPP branches and goes back into the glycolytic and gluconeogenic pathway to fructose 6-phosphate and glyceraldehyde 3-phosphate. For biosynthesis and redox regulation, the PPP generates R5P and NADPH. The oxidative and non-oxidative PPP enzymes are red-shaded (Redrawn from Ge et al., 2020). Created with BioRender.com.

1.2.3 Role of NADPH in PPP

F-6-P and G-3-P can also be obtained from the glycolysis step. Therefore, the shunting of G-6-P to PPP is primarily for the formation of NADPH. One of the primary functions of NADPH is the scavenging of ROS that is produced from oxidative phosphorylation in the mitochondria (please see the next section for more details).

The activation of the PPP is also necessary for biomass production. Thus, the ribose-5-phosphate formed during PPP is used to generate nucleotides in proliferating cells. NADPH is also consumed for the anabolic reaction of fatty acid synthesis (FAS) in cancer cells (Riganti *et al*., 2012). NADPH mainly provides reducing electrons for fatty acid synthase (FASN), a key rate-limiting enzyme, to synthesize fatty acids with acetyl-CoA as a primer and malonyl-CoA as a two-carbon donor. NADPH also provides the required electrons for the assembly of iron-sulfur (Fe/S) proteins involved in non-essential amino acid biosynthesis and lipoic acid synthesis, tRNA modification, telomere maintenance, and finally, DNA replication and repair (Ju *et*

al., 2020). Fatty acid synthetase is highly expressed in transformed cells; therefore, fatty acid synthetase has been considered as a target for developing drugs (Wongtangtintharn *et al*., 2004). Therefore, the flow of glucose into PPP creates a significant metabolic adaptation that can be exploited by multiple pathways in human cancer (Cho *et al*., 2018).

1.2.4 The Importance of NADPH Generation in Cancer Cells

NADPH is a major electron donor for reducing reactions in the metabolic process. Although many pathways are known to generate NADPH, according to quantitative flux analysis, NADPH is primarily generated via mitochondrial serine-driven one-carbon metabolism entering in folate-methionine cycles and cytosolic oxidative PPP (Locasale, 2013, Fan *et al*., 2014). G-3-P generates 30-40% of NADPH during serine generation in the presence of adequate nutrients. Most of the generated NADPH is used by proliferating cells for DNA synthesis and FAS (Fan *et al*., 2014). Depending on the tissue, 5-30 % of glucose enters the PPP flux (Riganti *et al*., 2012). When sufficient glucose is available, non-dividing cells use NADPH mainly for the FAS process. Consequently, in the liver, adipose tissue, adrenal glands, lactating mammary glands, and red blood cells, PPP is highly preferred (Cabezas *et al*., 1999, Riganti *et al*., 2012). As the main source of NADPH, the basal rate of the PPP flux is closely associated with the $NADP^+$/NADPH ratio. Moreover, the activity of the enzyme G6PD, which converts glucose-6-phosphate to 6-phosphogluconolactone, relies on the presence of a high $NADP^+$/NADPH ratio and converts $NADP^+$ to NADPH.

Via the NADPH-dependent enzymes glutathione reductase (GR) and thioredoxin reductase (TrxR), NADPH plays a crucial role in preserving the antioxidant pools of reduced glutathione (GSH) and thioredoxin (Trx). GSH and Trx are redox cofactors of cellular thiol that participate in redox-sensitive signaling pathways, scavenging hydroperoxides and enabling cellular redox potential to be retained. GSH and Trx can be oxidized in the presence of ROS by the enzymes glutathione peroxidase and

peroxiredoxin, respectively (Gauthier *et al*., 2013) (Figure 3). Studies have shown that these antioxidant mechanisms are upregulated in cancer cells compared to matched normal cells. In this respect, up-regulation of GSH and Trx in breast and prostate cancer was shown to be associated with the progression of the disease and poor patient outcomes (Ceccarelli *et al*., 2008, Cha *et al*., 2009). Due to the role of the PPP in protecting cells from oxidative stress, the flux of glucose through the PPP is highly relevant for human diseases. G6PD is expressed more in cancer cells than normal cells (Bokun *et al*., 1987). The tumor suppressor p53 was shown to restrict the activity of G6PD by reacting with it directly; thus, PPP flux and NADPH production rate were shown to be reduced (Jiang *et al*., 2011).

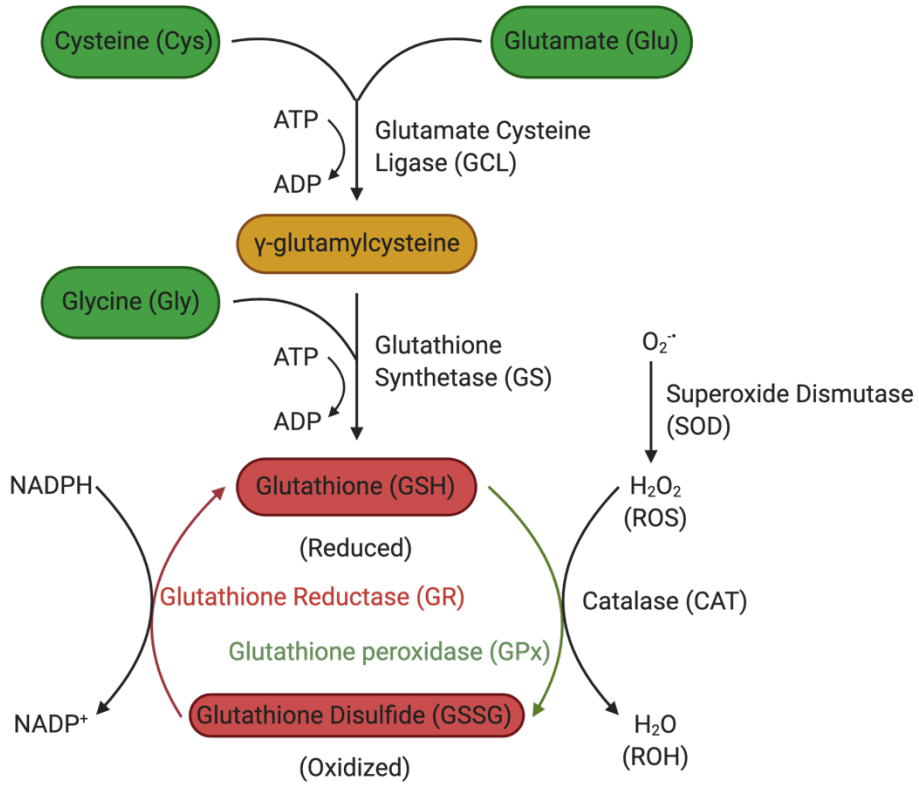

Figure 3. *Glutathione (GSH) redox cycle*

In a two-step pathway involving energy from ATP, glutathione (GSH) is synthesized from the amino acids glutamate (Glu), cysteine (Cys), and glycine (Gly). Via the action of glutamate-cysteine ligase (GCL), Glu and Cys are combined. This dipeptide then reacts with Gly via a glutathione synthetase reaction (GS). GSH

undergoes a redox reaction to detoxify reactive oxygen species (ROS) such as hydrogen peroxide, using glutathione peroxidase (GPx). The primary source of H_2O_2 is superoxide anion ($O_2^{\cdot-}$) conversion through the enzymatic action of superoxide dismutase (SOD). The enzymatic reaction of glutathione reductase (GR), which includes the cofactor nicotinamide adenine dinucleotide phosphate (NADPH) to form a redox cycle, converts GSH to an oxidized form (GSSG) and is recycled back to GSH (Redrawn from Simpson et al., 2015). Created with BioRender.com

1.3 Aldo-Keto Reductases

The Aldo-Keto Reductase (AKR) superfamily consists of several structurally related enzymes of common ancestry that catalyze redox transformations involved in biosynthesis, intermediary metabolism, and detoxification. Substrates of these enzymes include glucose, steroids, end products of glycosylation, products of lipid peroxidation, and environmental pollutants. The $(\beta\alpha)_8$ or Triose-phosphate isomerase (TIM)-barrel motif of these proteins is a compact but adaptable scaffolding with structural variations that can bind to a chemically diverse range of carbonyl substrates (Jez *et al*., 1997). Most AKRs catalyze simple oxidation-reduction reactions using NADPH as the cofactor (Figure 4). The enzymes are evolutionarily ancient, with fungi, plants, and animals expressing multiple AKR genes. AKR proteins have also been identified in a large variety of microorganisms (Ellis *et al*., 2002).

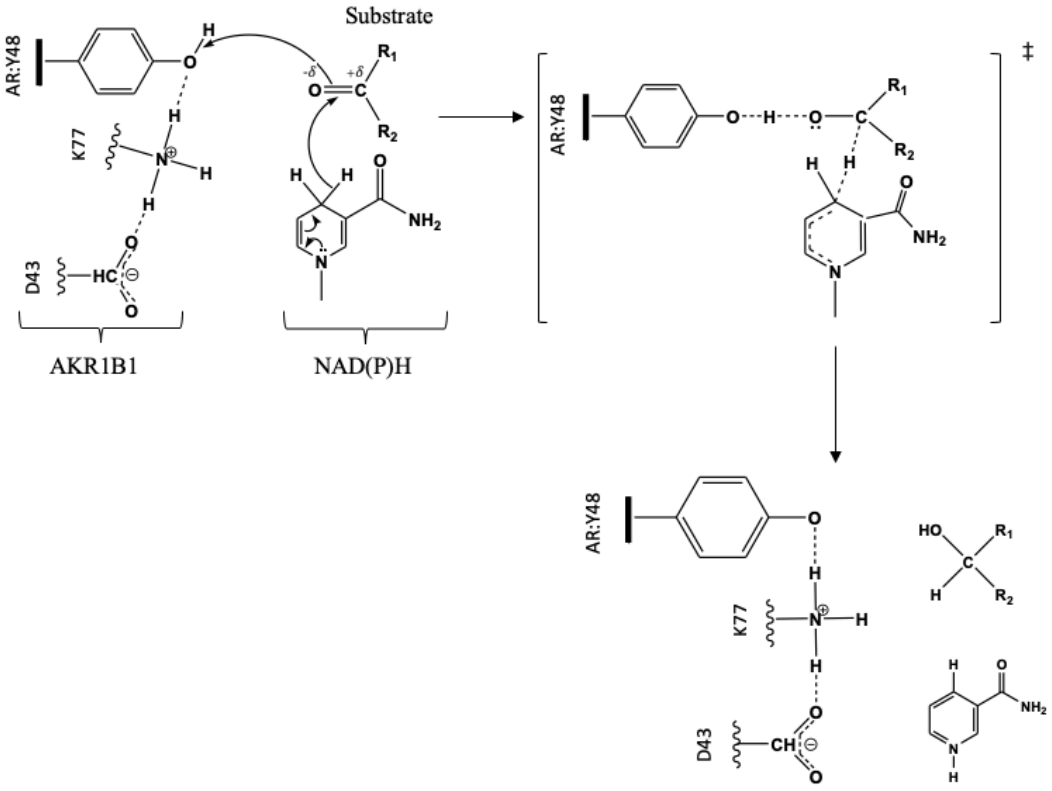

Figure 4. *The catalytic activity of AKR1B1*

Active site Tyr-48 (AKR1B1 numbering) is shown in the first complex to form a hydrogen bond with the carbonyl substrate, resulting in carbonyl polarization and accelerating the hydride transfer of the pro-R hydrogen from the NADPH nicotinamide ring to the substrate carbonyl carbon. The hydrogen bond network given by Lys-77 and Asp-43 is used to lower the tyrosine pKa, making it easier to transfer protons. The second complex indicates a transition state in which the proton transferred from protein tyrosine is quenched by polarization at the carbonyl and a concerted hydride transfer to the carbonyl carbon. The reduced carbonyl then dissociates from the acid-base catalyst, and the hydrogen-bonding network in the final complex stabilizes a net charge on the tyrosinate anion (Redrawn from Barski et al., 2008).

Oxidation-reduction reactions such as the reduction of glucose, glucocorticoids, small carbonyl metabolites, glutathione conjugates, and phospholipid aldehydes are catalyzed by proteins encoded by the AKR genes. In this ability, AKRs act as independent metabolic units or as interconnected metabolic pathway components in

which these enzymes work together with other carbonyl metabolizing enzymes such as glutathione S-transferases (GSTs), aldehyde dehydrogenases, alcohol dehydrogenases, and cytochrome P450s (CYPs). Given the variety of biological aldehydes that can potentially act as substrates for these enzymes, the transformation and detoxification of aldehydes and ketones formed endogenously during metabolism or found in the environment as nutrients, food, drugs, or toxins are likely to be the most essential function of the AKR superfamily (Bachur *et al*., 1976).

NADPH is favored over NADH by most AKRs as a cofactor. As indicated above, NADP is primarily available in the reduced form (as NADPH) in metabolically active cells (Pollak *et al*., 2007). A high NADPH/NADP+ ratio represents the cell's synthetic potential and is dissociated kinetically and thermodynamically from the NAD+/NADH ratio, which is mostly regulated by glycolysis and respiration rates. AKRs can, therefore, accomplish their metabolism and detoxification tasks without being impaired by cofactor ratio fluctuations due to changes in metabolic rate and ability. Therefore, the constant supply of NADPH sustained at high levels from the various NADPH generating pathways provides a strong driving force for AKRs to catalyze reductions in a wide range of cell energy states associated with different levels of respiration, reproduction of development, or starvation (Barski *et al*., 2008).

Fifteen AKR proteins have been identified in humans to date. These include AKR1A1 (aldehyde reductase), AKR1B1, AKR1B10 and AKR1B15 (aldose reductases), AKR1C1, AKR1C2, AKR1C3, and AKR1C4 (hydroxysteroid dehydrogenases), AKR1D1 (Δ4-3-ketosteroid-5-β-reductase), AKR1E2, AKR6A3, AKR6A5, and AKR6A9 (Kvβ proteins), and AKR7A2 and AKR7A3 (aflatoxin reductases) (Nishinaka *et al*., 2003, Barski *et al*., 2008, Weber *et al*., 2015).

1.3.1 Aldose Reductases (AKR1B1 and AKR1B10)

1.3.1.1 AKR1B1

AKR1B1 is by far the most studied AKR due to its possible function in mediating hyperglycemic injury and secondary diabetic complications (Dvornik *et al*., 1973, Gabbay *et al*., 1966). It catalyzes the elimination of low levels of glucose under baseline conditions. During hyperglycemia, increased glucose availability leads to an AKR1B1 mediated reduction of glucose to fructose and then to sorbitol (Figure 5). Increased sorbitol levels can lead to tissue injury; therefore, inhibition of AKR1B1 has been shown to prevent, postpone, or even reverse diabetes-related tissue injury (Gabbay, 2004, Dvornik *et al*., 1973, Nicolucci *et al*., 1996, Bril and Buchanan, 2006). According to NCBI (https://www.ncbi.nlm.nih.gov/variation /view/?q=rs5060&assm=GCF_000001405.38), the AKR1B1 gene has 5223 Single-Nucleotide Polymorphisms (SNPs), but none of these SNPs have been reported to contribute to a disease state.

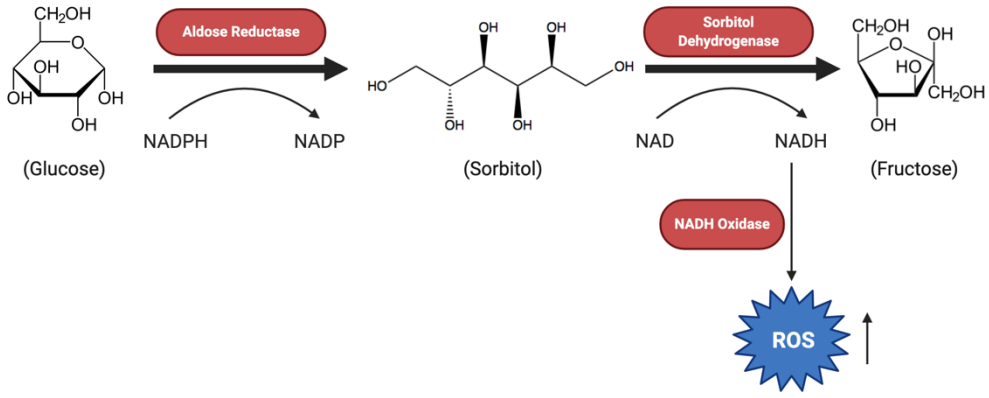

Figure 5. *Polyol pathway*

(Redrawn from Tang et al., 2012). Created with BioRender.com

AKR1B1 activity has been shown to be closely related to multiple inflammatory pathways. The use of AKR1B inhibitors has been shown to disrupt inflammation

caused by high glucose or cytokines such as TNF-alpha, leading to mitigation of injury (Ramana *et al*., 2007, Ramana *et al*., 2005, Ramana *et al*., 2003, Ramana *et al*., 2006). However, the mechanisms by which AKR1B1 controls these pathways remain unclear. The AKR1B1 protein itself is susceptible to oxidation via a hyperreactive cysteine residue found at the active site of the enzyme (Cys-298). Oxidation of this cysteine enhances catalysis and prevents inhibitor binding (Petrash *et al*., 1992). It has been proposed that this increase in enzyme activity is due to a reduction in enzyme affinity for NADPH (Ehrig *et al*., 1994). Since enzyme oxidation affects catalysis and substrate choice and may be caused by NO and peroxynitrite, it has been proposed that NO can regulate the polyol pathway and the function of AKR1B1 in inflammation, cell growth, and apoptosis (Ramana *et al*., 2003, Kaiserova *et al*., 2008).

1.3.1.2 AKR1B10

As opposed to the ubiquitously expressed AKR1B1 (Hyndman and Flynn, 1998), AKR1B10 is expressed predominantly in the small intestine, colon, liver, thymus, and adrenal gland (Cao *et al*., 1998). The amino acid sequence of AKR1B10 is 71% similar to that of AKR1B1; AKR1B10 also exhibits similar substrate specificity and inhibitor sensitivity as AKR1B1. Nonetheless, AKR1B10 shows several orders of magnitude more efficient catalysis of all-trans-retinal (Gallego *et al*., 2006), as well as many ketones, including drugs such as daunorubicin and dolasetron (Martin *et al*., 2006). AKR1B10 gene silencing using siRNA has been shown to result in growth inhibition and decreased foci formation rate and colony size of colorectal cancer cells, suggesting that AKR1B10 plays a critical role in the proliferation of cancer cells (Yan *et al*., 2007). The mitogenic function of AKR1B10 may be linked to retinoic acid depletion (due to excessive activity of AKR1B10) and subsequent loss of cell differentiation and cancer growth (Gallego *et al*., 2007). However, recent studies indicate that AKR1B10 has tumor-suppressive properties in CRC. Data from our lab indicates that CRC patients expressing high levels of AKR1B10 but low

levels of AKR1B1 in the colon showed longer disease-free survival (Taskoparan *et al*., 2017) and were predominantly classified as Consensus Molecular Subtype (CMS)-3 category, which was associated with an epithelial signature and metabolic deregulation (Demirkol *et al*., 2020). On the contrary, AKR1B10 protein is highly overexpressed in lung and hepatocellular carcinomas (Fukumoto *et al*., 2005; Cao *et al*., 1998) along with uterine cancer (Yoshitake *et al*., 2007). AKR1B10 expression in HCC has been related to Hepatitis-B virus (HBV) infection and is considered as a strong biomarker both for the detection of early HCC and for poor prognosis (Distefano & Davis, 2019, Wang *et al*., 2017). AKR1B10 appears to regulate fatty acid biosynthesis by interaction with the de novo synthetic pathway rate-limiting enzyme acetyl-CoA carboxylase-alpha (Ma *et al*., 2008), but the physiological significance of this function of AKR1B10 needs to be further investigated. It is also currently unclear why the expression of AKR1B10 is associated with poor outcomes in some tumor types and good outcomes in others. According to NCBI (https://www.ncbi.nlm.nih.gov/variation/view/?q=rs5060&assm=GCF_000001405.38), the AKR1B10 gene has 4445 Single-Nucleotide Polymorphisms (SNPs), but none of these SNPs have been reported to contribute to a disease state.

1.4 Metastasis

Recent data from our lab indicate that high expression of AKR1B1 was associated with increased motility in colon cancer cell lines (Taskoparan *et al*., 2017). Additionally, tumors expression high AKR1B1 but low AKR1B10 were significantly associated with a mesenchymal signature and predominantly belonged to the CMS4 category, associated with the mesenchymal phenotype (Demirkol *et al*., 2020). It is, however, mechanistically unclear how AKR1B1 or AKR1B10 modulate cellular motility or metastatic spread.

Metastasis is a complicated biological phenomenon that consists of multiple sequential and interrelated stages with mostly still obscure multi-biochemical events. Metastasis occurs essentially in four stages; detachment, migration, invasion, and

adhesion (Figure 6). This complex cascade is defined as an "invasion-metastasis cascade." In this cascade, new blood vessel development (angiogenesis), metastatic cell departure from the primary tumor (detachment and migration), invasion of the basement membrane (BM) and extracellular matrix (ECM) surrounding the tumor, invasion of the basement membrane (BM) which supports the endothelium of local lymphatic and blood vessels, metastatic cell intravasation into the lymphatic or blood vessels, circulating metastatic cell adhesion to the endothelium layer of capillaries of the target organ site, endothelial cell layer and surrounding basement membrane (BM) invasion and finally the settlement and growth of secondary tumors at the target organ site occurs (Daenen *et al*., 2011; Hu *et al*., 2012).

Cancer metastasis is responsible for about 90% of all cancer deaths and the primary cause of mortality and morbidity (Seyfield & Huysentruyt, 2013). With today's technological advances in early cancer detection and treatment, most solid tumors are now curable or manageable if the tumor is diagnosed prior to its metastatic spread. Metastatic tumors are highly incurable and fatal (Wells *et al*., 2013).

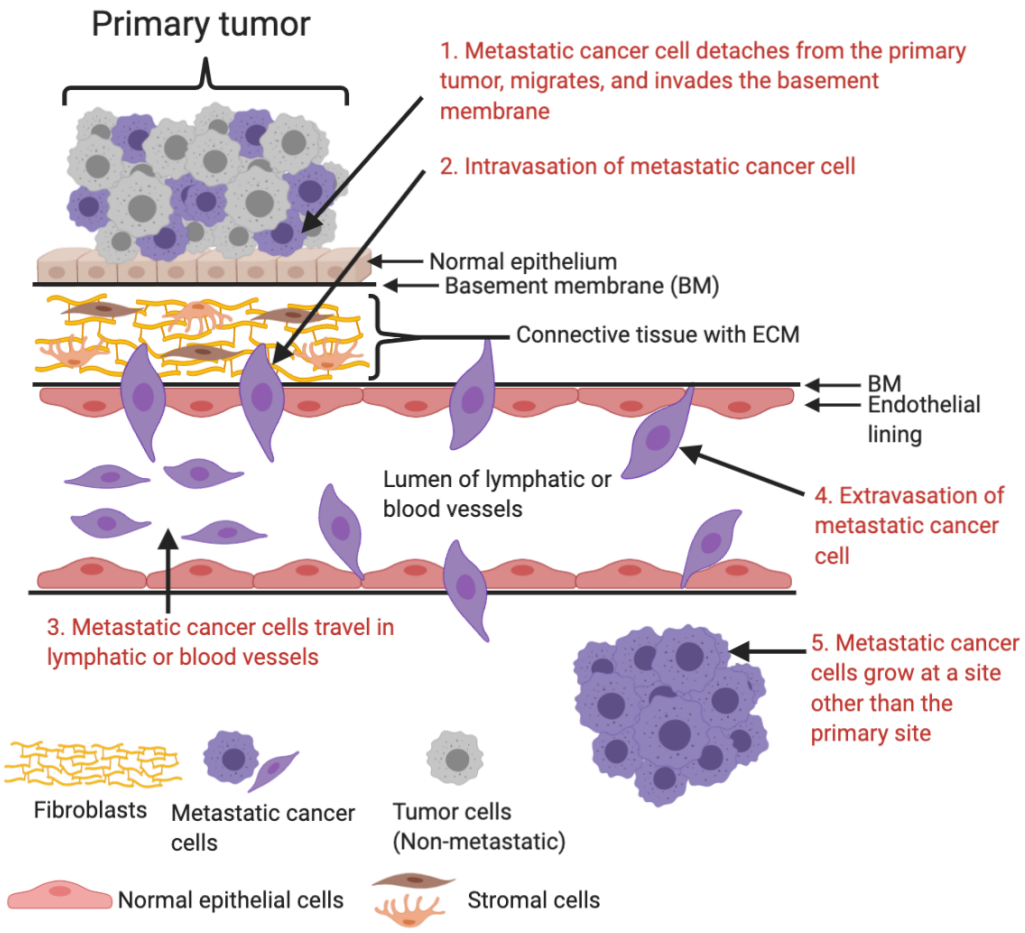

Figure 6. *Overview of the invasion-metastasis cascade*

(Redrawn from Cao et al., 2015). Created with BioRender.com.

In colorectal cancer (CRC), the most common distant metastasis sites are the peritoneum and the liver. Approximately 20% of patients have synchronous metastases present, most commonly in the liver, and nearly 60% of patients establish distant metastases in 5 years (Cook *et al*., 2005; Desch *et al*., 2005).

1.4.1 Epithelial-Mesenchymal Transition

A vital aspect of the metastatic spread of cancer cells is the Epithelial-Mesenchymal Transition (EMT). In EMT, epithelial cells lose their cell to cell adherence and gain mesenchymal properties, which are very important for invasion and metastasis. These mesenchymal properties include increased mobility and invasiveness, increased resistance to apoptosis, degradation, and extracellular matrix (ECM) components production (Cao *et al*., 2015). Different molecular levels regulate the EMT process (Figure 7).

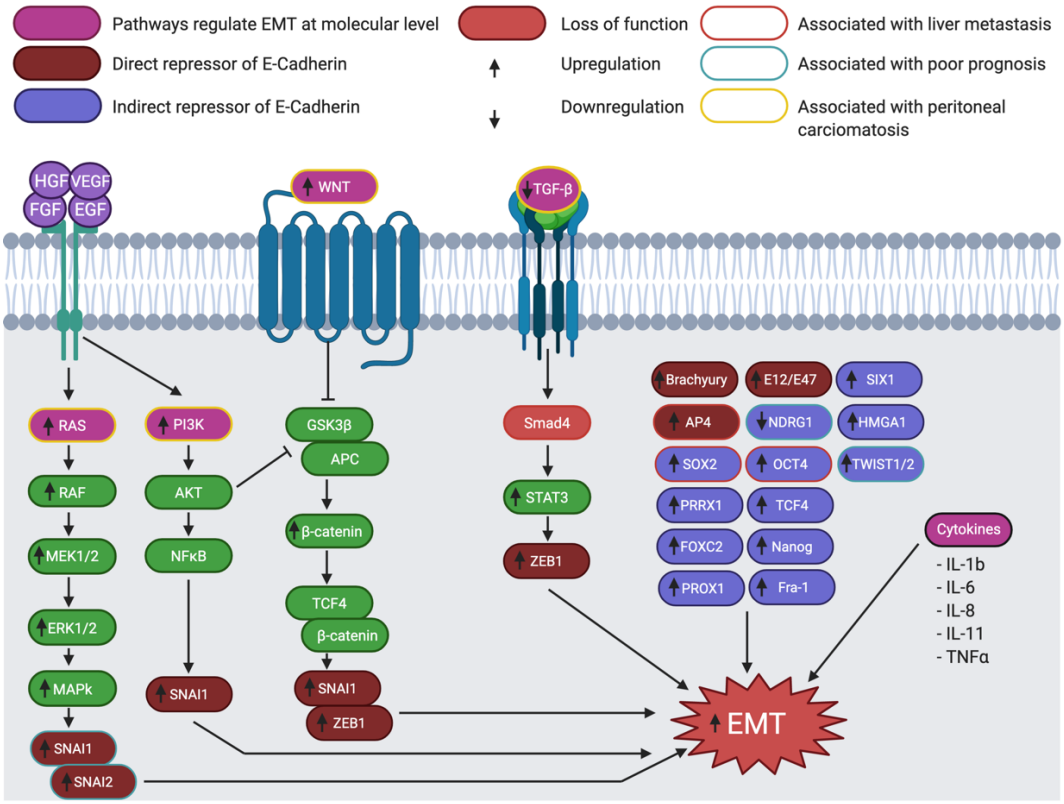

Figure 7. *Upregulation or downregulation of different molecular pathways and other molecules enhance EMT*

Downstream targets of these pathways downregulate E-cadherin directly or indirectly, which leads to the activation of EMT (Redrawn from Pretzsch et al., 2019) Created with BioRender.com.

The regulation of EMT is directly linked to the expression of the transmembrane protein E-Cadherin. E-cadherin plays an essential role in stabilizing cell to cell contacts, allowing the cell to sustain its epithelial state and maintain cell polarity. When E-Cadherin levels are reduced, it is generally followed by an upregulation of the non-epithelial adhesion molecule N-Cadherin. It is known that N-Cadherin promotes tumor progression by increasing ß-catenin activity and FGFR signaling (Van Roy, 2014). There are various transcription factors controlling E-cadherin expression in CRC. These transcription factors can be divided into two distinct groups; direct repressors and indirect repressors. Direct repressors act on E-Cadherin via directly binding to the promoter region. SNAIL (SNAI1,2), E12/E47, ZEB (ZEB1,2), AP4, and Brachyury are direct repressors of E-Cadherin. Most of these proteins are considered to be mesenchymal markers. Indirect repressors of E-Cadherin have multiple specific targets. These transcription factors regulate E-Cadherin transcription at different levels, which also involves activation of direct E-Cadherin repressors. TWIST (TWIST1,2), TCF4, FOXC2, SOX2, Nanog, OCT4, PROX1, PRRX1, SIX1, Fra-1, and HMGA1 are the indirect repressors of E-Cadherin (Pretzsch *et al*., 2019).

1.5 Hypothesis and Aims of the Study

Our lab has recently reported that the AKR1B1 mRNA expression in colon and rectum tumor specimens from 52 patients was highly significantly and strongly positively correlated with the expression of the mesenchymal marker Vimentin and significantly and negatively correlated with the expression of the epithelial marker E-cadherin (Demirkol *et al*., 2020). A reverse relationship was observed with the mRNA expression of AKR1B10. It is currently unknown mechanistically how the high expression of AKR1B1 leads to a mesenchymal phenotype while high expression of AKR1B10 leads to an epithelial phenotype. To address this, I aimed to utilize *in vitro* tools to better understand the functional changes that occur upon overexpression of AKR1B1 or AKR1B10 in the CRC cell line that does not express

either gene. I examined the hypothesis that overexpression of AKR1B1 or AKR1B10 may have significant effects on energy metabolism and cellular motility in CRC cell lines.

CHAPTER 2

MATERIALS AND METHODS

2.1 Cell Culture

The colorectal cancer (CRC) cell line SW480 was purchased from American Type Culture Collection (ATCC) (Middlesex, UK). HEK293FT cell line was kindly gifted by Dr. Mayda Gürsel (Middle East Technical University, Turkey). AKR1B1 or AKR1B10 overexpressing stable polyclonal SW480 cell lines and the empty vector (EV) control cells were generated by İsmail Güderer, a graduate student in our lab, with a lentiviral transduction method. SW480 cells were grown in Leibovitz L-15 Medium (Biological Industries, Israel) supplemented with 10% fetal bovine serum (FBS) and 1% Penicillin-Streptomycin in a humidified incubator with 100% air at 37ºC. Plastic consumables used in cell culture were purchased from Sarstedt (Germany).

SW480 cells were originally isolated from a patient with Duke's B colorectal adenocarcinoma. These cells are classified as microsatellite stable and contain a G12V *KRAS* mutation, R273H and P309S mutations in *TP53* and wild type BRAF, PIK3CA, and PTEN (Ahmed *et al.,* 2013). SW480 cells also do not express any AKR1B1 or AKR1B10 within the detectable limits of western blot or RT-qPCR and therefore were suitable for the overexpression of both AKR1B1 and AKR1B10. Additionally, the culture medium of SW480 cells contains galactose as the primary source of energy, rather than glucose. As AKRs are known to be active in the presence of glucose, we reasoned that the use of these cells could provide us data on the activation of the AKR pathway in the absence of glucose.

2.2 Overexpression of AKR1B1 and AKR1B10 in SW480 cells

The AKR1B1 and AKR1B10 cDNAs cloned into the pLenti-Puro plasmid was available in our lab. EcoRI and XbaI restriction enzymes were used to digest the pLenti-puro plasmid. Cloning of AKR1B1 (NM_001628) and AKR1B10 (NM_020299) cDNA sequences into pLenti-puro vector was carried out by Esin Gülce Seza, a graduate student in our lab. Confirmation of the cloning was carried out by sequencing (BMLabosis, Ankara). The transfection reagent of choice as polyethyleneimine (PEI) at a ratio of 1:3 w/v [DNA (µg) to PEI (1mg/ml) (µl)]. HEK293FT cells were seeded to 10 cm cell culture dishes and allowed to proliferate for 24 h in order to reach 70% confluency. These cells were then co-transfected with psPax2 (packaging plasmid), p-CMV-VSV-G (envelope plasmid), and the pLenti-puro (transfer plasmid) containing AKR1B1 or AKR1B10 cDNA at the plasmid ratios of 2.5: 2.5:5 (psPax2, p-CMV-VSV-G, pLenti-puro, respectively). The viruses were collected at 48 and 72 h after transfection, snap-frozen in liquid N_2 (-160ºC), and stored at -80ºC. Viral transduction experiments were conducted by seeding 50,000 SW480 cells/well in a 12-well plate. After 24 h, the cells were treated with the collected viruses at a dilution of 1:1 [1 volume of lentivirus (µl) to 1 volume of complete medium (µl) + 10 µg/mL Polybrene (µl)]. Polybrene (Merck Millipore, Germany) was added to increase viral transduction efficiency (Abe *et al*., 1998). Cells were incubated for 72 h with virus-containing media and, after transduction, cultured with Puromycin (Invivogen, USA) containing complete media for selection. The selection step of the protocol was continued until all wild-type cells were dead. From 2.5 µl starting concentration to 1 µl concentration of Puromycin was used gradually in the selection step and media of the cells changed every day during this process. A kill curve was generated to determine the dosage of Puromycin by İsmail Güderer. Primary stocks of polyclonal cells were prepared with 5% DMSO containing medium after the selection step and stored in the vapor phase of liquid nitrogen for further use.

2.3 Protein Isolation & Quantification

Total protein isolation was carried out using Mammalian Protein Extraction Reagent M-PER (Thermo Fisher Scientific, USA) containing PhosSTOP Phosphatase Inhibitor and c0mplete Mini EDTA-free Protease Inhibitor Cocktail (Roche, Germany) according to the manufacturer's instructions.

Measurement of the isolated protein content was done by Bradford assay using Coomassie Protein Assay Reagent (Thermo Fisher Scientific, USA) and a standard curve generated with bovine serum albumin (BSA). 5 µl of total protein was added to 1.5 ml of Coomassie Protein Assay Reagent in a plastic cuvette and absorbance value was obtained by using Multiskan-GO microplate reader (Thermo Fisher Scientific, USA) at 595 nm. Quantified amount was later determined by applying the reading to a standard curve.

2.4 Western Blot

Western blot technique was used to confirm the expression of proteins of interest in the cell lines used. Total proteins were separated using reducing SDS-Polyacrylamide Gel Electrophoresis (SDS-PAGE) at 95 V by loading 30 µg protein per well in 10% Acrylamide/Bis-acrylamide gels. As a marker for the 10-250 kDa range, PageRuler Plus Prestained Protein Ladder (Thermo Fisher Scientific, USA) was used. Before separation, a wet-transfer of proteins from the gel to a Polyvinylidene Fluoride (PVDF) membrane was carried out at 115 V and 4 ºC for 75 minutes. Membrane blocking was conducted in TBS-T containing 5% skimmed milk. Primary antibodies were incubated overnight at 4ºC. The membranes were incubated with the primary antibody (Table 1) and then extensively washed with TBS-T, followed by incubation with the secondary antibodies at room temperature for 1 hour and then washed again with TBS-T. The membranes were next incubated with Clarity ECL Substrate (BioRad, USA) as the visualization agent for 1 min and imaged in a Chemi-Doc MP (BioRad, USA). When necessary, the membranes were

stripped by incubating in a mild stripping buffer for 10 minutes at 60ºC and washed extensively with TBS-T before reprobing with a different antibody. Alpha Tubulin or GAPDH antibody was used as a loading control to ensure equal protein loading.

Table 1. *Primary antibodies used in western blotting experiments with their properties*

Description	Size (kDa)	Catalog Number	Origin	Brand	Dilution	Medium
AKR1B1	35	PA5-29718	Rabbit	Thermo Fisher	1:500	5% skimmed milk
AKR1B10	35	PA5-23017	Rabbit	Thermo Fisher	1:500	5% skimmed milk
G6PD	58	12263S	Rabbit	Cell Signaling	1:1000	5% skimmed milk
Cyclin B1	60	sc-245	Mouse	Santa Cruz	1:500	5% skimmed milk
Alpha Tubulin	52	Proteintech HRP-66031	Mouse	Proteintech	1:5000	5% skimmed milk
GAPDH	37	sc-47724	Mouse	Santa Cruz	1:4000	5% skimmed milk

2.5 RNA Isolation

Total RNA isolation was conducted by using the NucleoSpin RNA Extraction Kit (Macherey-Nagel, Germany) according to the manufacturer's instructions on scraped cells. Approximately 500,000 cells were collected for the total RNA isolation procedure. NanoDrop (Biochrom, UK) was used for RNA quantification. A260/280 ratio close to 2.0 and A260/230 ratio between 2.0 and 2.2 were accepted as acceptable RNA samples. All samples were stored at -80ºC after isolation and quantification.

2.6 cDNA Synthesis

Total RNA samples were treated with RNase-free DNase I (Thermo Fisher Scientific, USA). 1 µg of RNA sample was used for each cDNA synthesis reaction with RevertAid First Strand cDNA Synthesis Kit (Thermo Fisher Scientific, USA). Random hexamers were used, and all reactions were conducted according to the manufacturer's instructions. Synthesized cDNA samples were stored at -20ºC.

2.7 qRT-PCR

To screen the expression of genes that utilize NADPH in cellular energetics pathways, quantitative real-time PCR (qRT-PCR) assay was used. Primers used in this study along with their NCBI reference sequences are given in Table 2 and Table 3. The final volume of the reaction was set to 10 µl and contained 1 µl of cDNA (1:10 diluted) and 9 µl reaction mix [0.5-1 µM of Forward and Reverse primers, 5 µl GoTaq qPCR Master Mix (Promega, USA) and dH_2O to complete the volume]. Standard curves were generated (with 1:10, 1:50, 1:100, 1:250, 1:500, 1:1000 and 1:10000 dilutions of 500 ng cDNA) for each primer pair for quantification. β-actin or GAPDH were used as internal controls. The reactions were carried out in Rotor-Gene Q (Qiagen, Netherlands) qRT-PCR equipment. Expression values of individual

genes were determined using the Pfaffl method, which implies relative quantification based on target genes and reference genes representing physiological differences in the expression level difference (Pfaffl, 2001).

Table 2. *Sequences and T_m values of primers*

Gene Name	Forward (5'-3')	Reverse (5'-3')	T_m (°C)
AKR1B1	AAGCCGTCTCCTGCTCA	TTGCTGACGATGAAGAGC	55
AKR1B10	CAGAATGAACATGAAGTGGGG	GCTTTTCCACCGATGGC	55
G6PD	TGACCTGGCCAAGAAGAAGA	CAAAGAAGTCCTCCAGCTTG	56
ACTB	CAGCCATGTACGTTGCTATCCAGG	AGGTCCAGACGCAGGATGGCATG	60

Table 3. *NCBI reference sequences of primers*

Gene Name	NCBI Reference Sequence
AKR1B1	NM_001628.4
AKR1B10	NM_020299.5
G6PD	NM_001042351.3, NM_001360016.2, NM_000402.4
ACTB	NM_001101.5, NM_001199954.3, NM_001614.5, NM_001613.4, NM_001141945.2, NM_001320855.1, NM_001083538.3, NM_001371926.1, NM_001277083.2, NM_001277406.2, NM_001099771.2, NM_005159.5, NM_001100.4, NM_001145442.1, NM_001017992.4

2.8 Proliferation Assay - MTT

To determine whether overexpression of AKR1B1 and AKR1B10 in the colon cancer cell line SW480 affected the proliferation of these cells, the MTT [3-(4, 5-dimethylthiazol-2-yl)-2, 5-diphenyltetrazolium bromide] assay was conducted according to the manufacturer's instructions (Sigma Aldrich, USA). 7,500 cells per well [5-10 replicates each for AKR1B1 and AKR1B10 overexpressing SW480 cells and empty vector (EV) transfected cells] were seeded in each well of three independent 96 well plates to determine the proliferation at three different time points (24-48-72 hours). At the end of each time point, 10% MTT (dissolved in PBS) containing 100 µl medium was applied directly into the cells to enable the formation of formazan crystals in the metabolically active (and thereby proliferating cells). After 4 hours of incubation, 1% SDS-0.01M HCl was introduced to each well to solubilize the formazan crystals. Each plate was then incubated for 16 hours at 37°C in a humidified incubator. The absorbance values at 570 nm from each well were determined using a Multiskan-GO microplate reader (Thermo Fisher Scientific, USA).

2.9 Colony Formation Assay

To determine the effects of AKR1B1 or AKR1B10 overexpression on colony formation capacity and long term proliferative rate of SW480 cells, a colony formation assay was carried out according to previously published protocols (Feoktistova *et al*., 2016). SW480 cells were seeded to 6 well plates at a density of 1,000 cells/well. Then cells were cultured for 10 days in a humidified incubator with 100% air at 37ºC when the colonies became visible to the naked eye. Cells were washed with PBS once and fixed with 4% Paraformaldehyde (PFA) solution (Sigma Aldrich, USA) for 15 minutes at room temperature. Following the fixation process, the PFA solution was removed from the wells, and cells were rewashed with PBS once. After this step, 1 ml of 0.5% crystal violet (dissolved in methanol) solution

(Sigma Aldrich, USA) was applied directly to the wells and incubated for 20 minutes at room temperature on a bench-type rocker. Next, plates were carefully washed with a gentle stream of tap water 4 times and left to air-dry overnight without a lid. The next day, stained colonies were imaged by using Chemi-Doc MP (BioRad, USA). Obtained images were analyzed with ImageJ (NIH, USA) software Threshold/Subtract method.

2.10 Spheroid Formation Assay

To determine the capacity of AKR1B1 and AKR1B10 overexpressing SW480 cells to form spheroids in 3D cell culture and to determine their size, as well as tightness, a spheroid formation assay was carried out. Empty vector (EV), AKR1B1, and AKR1B10 transduced cells were seeded in 10,000 cells/well density to 96 well Ultra-Low Attachment (ULA) plates (Corning, USA) and cultured in a humidified incubator with 100% air at 37ºC for 5 days. After culturing, each individual spheroid formed in the 96 well ULA plate was imaged and analyzed for their area by using the edge-detection/thresholding method on ImageJ software.

2.10.1 Live-dead Staining Cell Viability Assay

For determining the viability of the AKR1B1 and AKR1B10 overexpressing SW480 spheroids in 3D culture, live-dead staining cell viability assay was carried out. Empty vector (EV), AKR1B1, and AKR1B10 transduced cells were seeded in 10,000 cells/well density to 96 well Ultra-Low Attachment (ULA) plates (Corning, USA) and cultured in a humidified incubator with 100% air at 37ºC for 5 days. After culturing, spheroids were stained with Calcein-AM (0.5 µl/ml) for live cells and with ethidium homodimer-1 (2 µl/ml) for dead cells according to the manufacturer's instructions (Thermo Fisher Scientific, USA). Stained samples were imaged with Zeiss LSM 800 Laser Scanning Microscope (Germany) and obtained images were analyzed by using the edge-detection/thresholding method on ImageJ software.

2.11 Wound Healing Assay

To assess the motility differences between AKR1B1 or AKR1B10 overexpression in SW480 cells wound healing assay was carried out. Empty vector (EV), AKR1B1, and AKR1B10 transduced cells were seeded in 1,000,000 cells/well density to 6 well plates and cultured in a humidified incubator with 100% air at 37ºC to confluency. After reaching confluency, cells were washed with PBS once, and 1 ml of fresh PBS was added to each well. Wounds were created in each well by using a 100 µl pipette tip. After this step, PBS was aspirated, and 0.5 µM Mitomycin C (Serva Biochemicals, Germany) containing complete media were introduced to each well. Mitomycin C was used to inhibit proliferation. Cells were imaged every 24 hours for a total time of 72 hours. Obtained images were analyzed by the edge-detection/thresholding method on ImageJ software.

2.12 Cell Cycle Assay

To investigate whether AKR1B1 or AKR1B10 overexpression in SW480 cells affected cell cycle progression, PI (Propidium Iodide (Sigma Aldrich, USA)) assay was performed using flow cytometry. Before the assay, cells were synchronized by 16 hours of serum starvation with FBS-free medium. After the synchronization, one set of cells were collected as control, and the second set was released from synchronization by replacing the medium with complete medium. Released cells were collected after 8 hours, counted, adjusted to 40,000 cells/sample, and washed once with PBS. To fix the cells, 1.0 ml of ice-cold ethanol (70% percent) was introduced to the cells dropwise and vortexed gently. After 2 hours of incubation at -20ºC, the cells were centrifuged at 400 x *g* for 5 minutes. Then all the ethanol was removed carefully, and the pellet was washed with PBS and centrifuged at 400 x *g* for 5 minutes. After removing all PBS, cells were next incubated with the PI staining solution (0.1% Triton X-100, 2 mg/ml DNAse free RNase A, 1mg/ml PI) in the dark for 30 minutes at room temperature. The cells were then analyzed for cell cycle

progression in an Accuri C6 Flow Cytometer (BD Biosciences, USA). Cell cycle synchronization controls were included and also analyzed by SSC (Side Scatter), FSC (Forward Scatter), and the FL-3 channel in BD Accuri™ C6 Plus Analysis Software (BD Biosciences, USA).

2.13 Statistical Analysis

All experiments were carried out with at least two or three independent biological replicates and each biological replicate contained at least three technical replicates. GraphPad Prism 6.1 Software (GraphPad Software Inc., USA) was used to perform statistical analyses and generate graphs. One-way ANOVA, Two-way ANOVA, and Student's t-Test were used to determine statistical differences between experimental groups. A p-value of <0.05 was considered statistically significant.

CHAPTER 3

RESULTS

In this thesis, we aimed to investigate the effects of AKR1B1 and AKR1B10 overexpression on colorectal cell line SW480. Previous studies from our lab showed us that the expression profile of these aldose-reductases are significant in the progression and prognosis of CRC (Taşkoparan *et al*., 2017). Recent findings from our lab also indicate the presence of a correlation between AKR expression in fresh-frozen colorectal tumor specimens and their EMT status (Demirkol *et al*., 2020). Briefly, high expression of the AKR1B1 was accompanied by a high expression of the mesenchymal marker Vimentin and low expression of the epithelial marker E-cadherin. On the other hand, high expression of AKR1B10 was accompanied by a high expression of E-cadherin and low expression of Vimentin. In the light of these findings, we aimed to conduct functional assays to assess the effect of AKR1B1 or AKR1B10 overexpression in a cell line that does not endogenously express either protein *in vitro* and evaluate the signaling pathways involved.

3.1 Generation of AKR1B1 or AKR1B10 overexpressing SW480 cell lines

To investigate the effects of AKR expression, first, AKR1B1 and AKR1B10 overexpressing SW480 cells were generated. A lentiviral transduction method was chosen in order to obtain stable AKR1B1 or AKR1B10 expressing cells. Esin Gülce Seza, a graduate student in our lab, generated pLenti puro plasmids containing AKR1B1 or AKR1B10 overexpression sequences. Next, İsmail Güderer, also a graduate student in our lab, used these plasmids to generate lentiviruses for transduction. SW480 cells were transduced with these lentivirus particles to overexpress AKR1B1 or AKR1B10 genes and selected with Puromycin to generate polyclonal stable overexpressing cell lines. The generated cell lines were confirmed

for overexpression with qRT-PCR (Figure 8) and western blotting (Figure 9A and B).

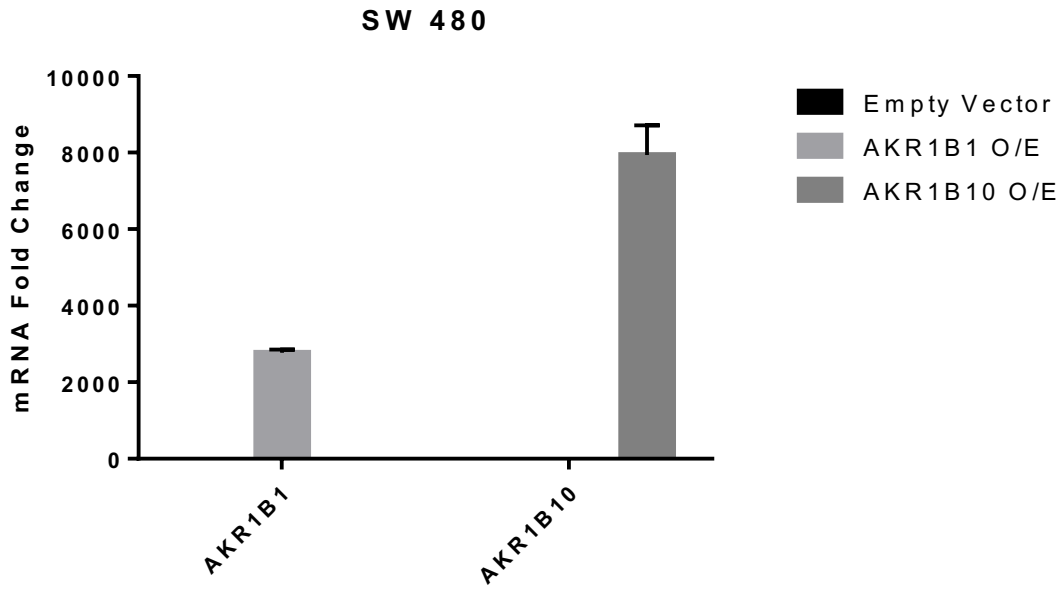

Figure 8. *Confirmation of AKR1B1 or AKR1B10 mRNA overexpression in SW480 cells with qRT-PCR*

To confirm the effects of lentiviral transduction on SW480 cells, qRT-PCR assay was conducted. 1 µg of sample cDNA was used in 1:5 dilution for each reaction with 3 internal replicates. Reactions were conducted in 40 cycles. B-actin was used as an internal control for qRT-PCR. Obtained data were normalized to B-actin and analyzed by using the Pfaffl method (Pfaffl, 2001). In order to perform this analysis, Ct values of AKR1B1 and AKR1B10 in Empty Vector (EV) transduced cells were accepted as 40. These cell lines were kindly generated by Ismail Güderer.

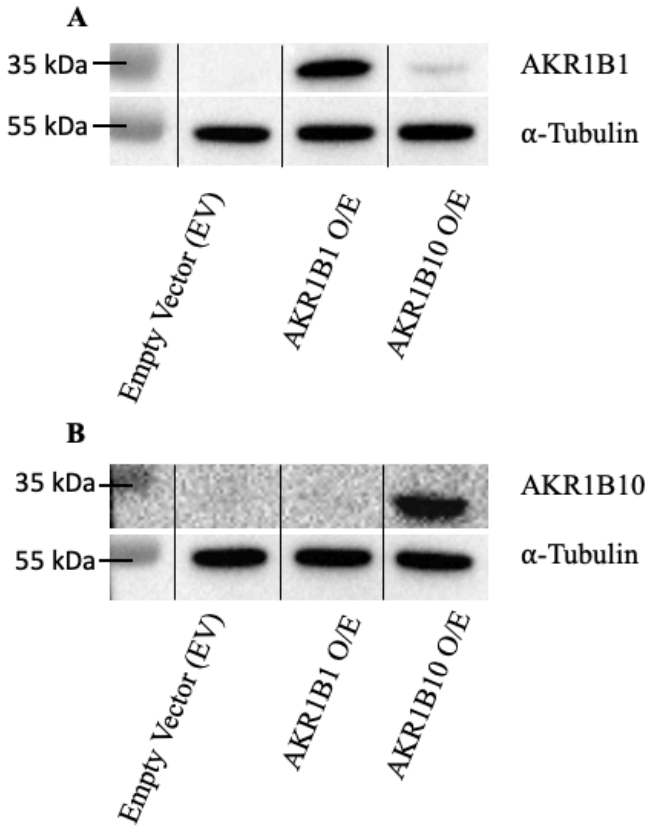

Figure 9. *Confirmation of overexpression of AKR1B1 or AKR1B10 protein in SW480 cells with western blotting*

To confirm the overexpression of AKR1B1 and AKR1B10 in SW480 cells, western blotting assay was conducted. 15 µg of total protein was loaded to 10% Acrylamide/Bis-acrylamide gel and wet-transferred to a PVDF membrane. Confirmation was carried out in two separate westerns; (A) AKR1B1 polyclonal antibody was blotted, (B) AKR1B10 monoclonal antibody was blotted. α-Tubulin antibody was used as loading control. These cell lines were kindly generated by Ismail Güderer.

As seen from Figure 9A, the AKR1B1 primary antibody also tends to recognize AKR1B10, albeit with very weak specificity compared to its ability to bind to AKR1B1. The AKR1B10 antibody was more specific and did not show any cross-reactivity with AKR1B1.

3.2 Effects of AKR1B1 and AKR1B10 overexpression on cellular proliferation in SW480 cells

To investigate whether overexpression of AKR1B1 or AKR1B10 affected the proliferation of SW480 cells, an MTT assay was carried out for 24 - 72 hours. Wild-type, empty vector (EV), AKR1B1, or AKR1B10 overexpressing cells were used in this assay (Figure 10). Wild-type and EV cells were used as controls. No significant change was observed between the samples suggesting that the overexpression of AKR1B1 or AKR1B10 did not impinge on proliferative signaling.

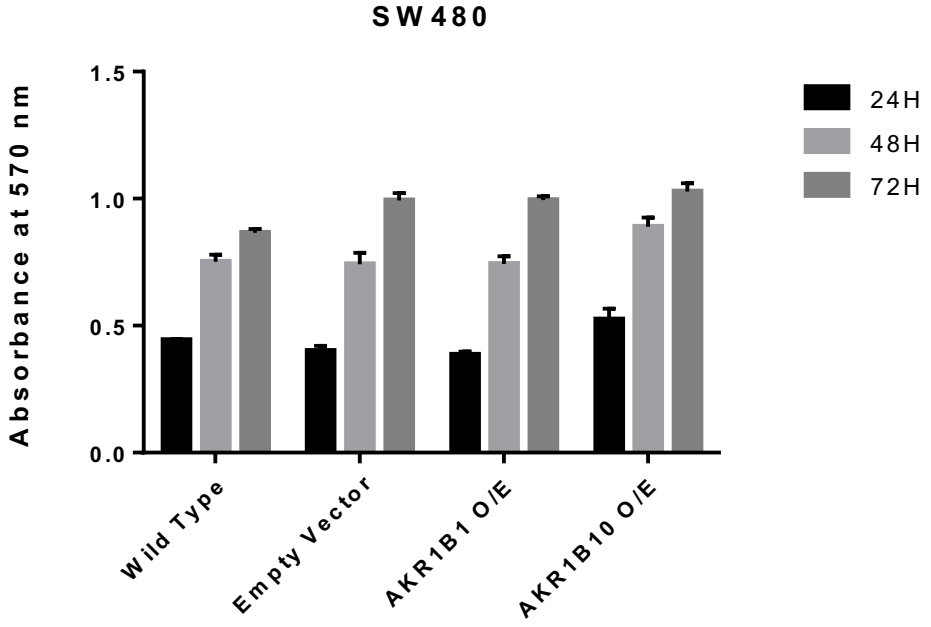

Figure 10. *Effects of AKR1B1 and AKR1B10 lentiviral transduction on cell proliferation using MTT assay*

SW480 wild type, empty vector (EV), AKR1B1 overexpressing, and AKR1B10 overexpressing cells were seeded to 96 well plates at 7,500 cells/well density. After overnight attachment of the cells, the plates were incubated for 24-72h. At the end of the incubation period, the medium was replaced with 10% MTT-containing medium and incubated for 4 hours. 1% SDS-0.01M HCl solution was then directly

added for the solubilization of formazan crystals for 16h, and the absorbance was measured in a microplate reader at 570 nm. No significant change in proliferation was observed with the overexpression of AKR1B1 and AKR1B10 compared to empty vector (EV) or wild type cells (controls). Two independent biological replicates were carried out.

For further investigation, a more extended time point colony formation assay was carried out. In this assay, cells were cultured to form colonies over 10 days and then stained with crystal violet for visualizing and counting the number of colonies formed. Colony formation assay showed a significant difference between the proliferative rate of EV and AKR1B10 overexpressing cells (Figure 11).

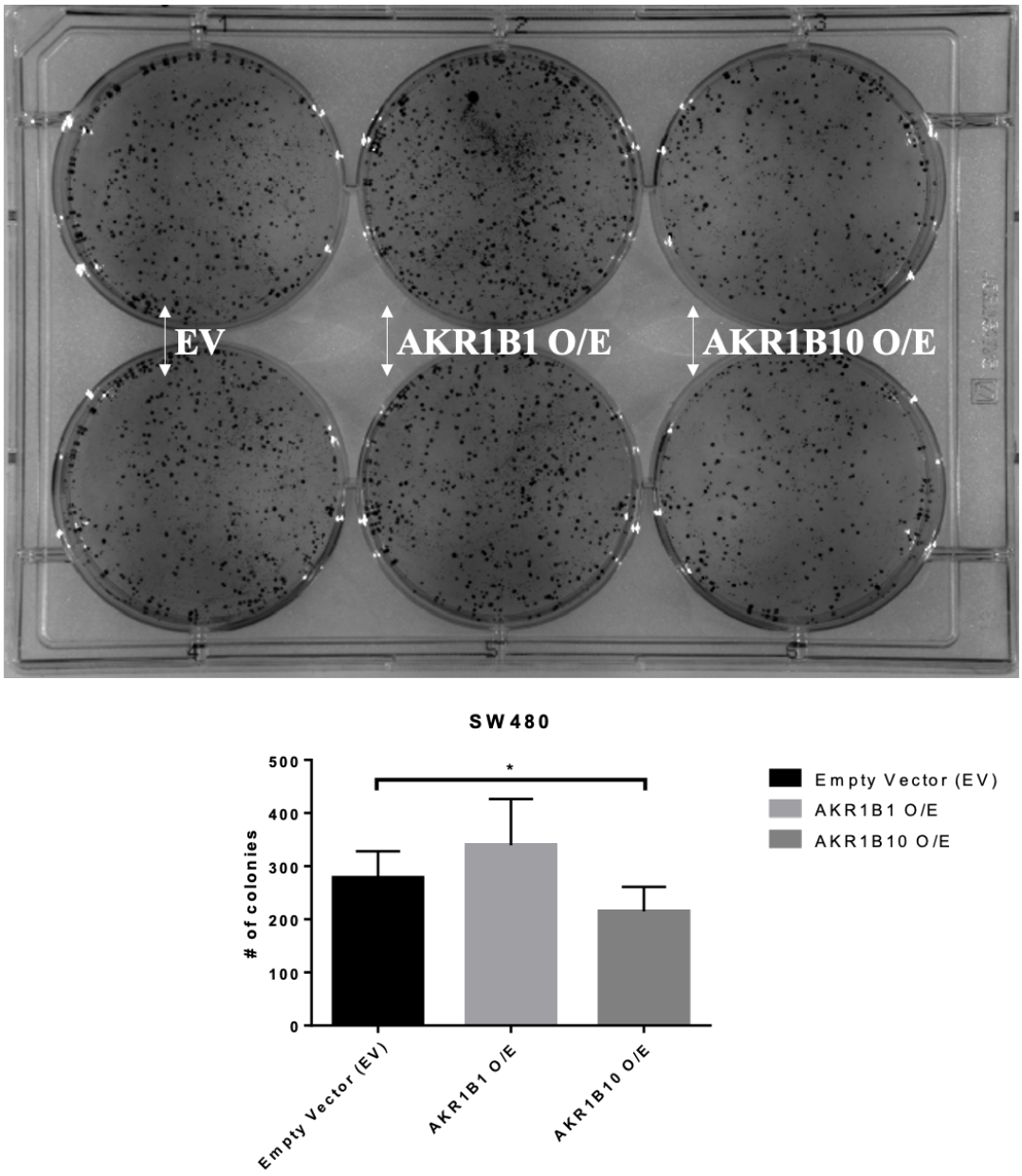

Figure 11. *Effects of AKR1B1 and AKR1B10 lentiviral transduction on cell proliferation using colony formation assay*

*SW480 empty vector (EV), AKR1B1 overexpressing, and AKR1B10 overexpressing cells were seeded to 6 well plates at 1,000 cells/well density. Cells were cultured for 10 days to promote colony formation and then stained with 0.5% crystal violet solution for visualization. Counting of colonies was done by edge-detection/thresholding method on ImageJ software. Two independent biological replicates were used for statistical analysis. Significance was determined by Two-way ANOVA. *p<0.05, **p<0.01.*

Finally, to assess the effect of AKR1B1 and AKR1B10 overexpression on proliferation in 3D culture conditions, spheroid formation assay was conducted (Figure 12). Cells were cultured in a 96 well ULA plate for 5 days, and the results showed that there is a significant difference between the size of spheroids formed in AKR1B1 overexpressed cells compared to the empty vector (EV) transfected cells.

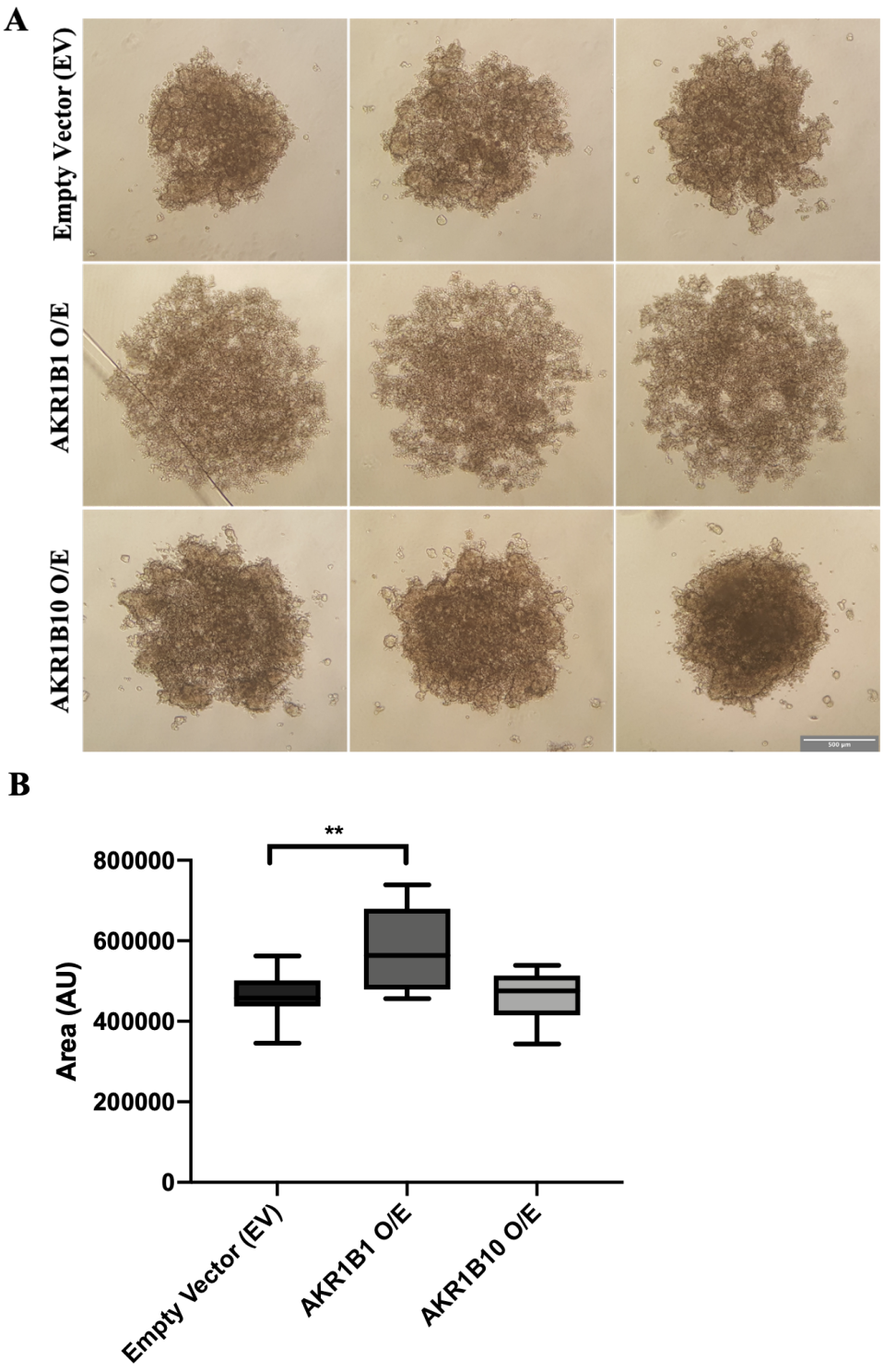

Figure 12. *Effects of AKR1B1 and AKR1B10 lentiviral transduction on 3D cell culture using spheroid formation assay*

*SW480 empty vector (EV), AKR1B1 overexpressing, and AKR1B10 overexpressing cells were seeded to 96 well ULA plates at 10,000 cells/well density and cultured for 5 days to promote spheroid formation. After 5 days, spheroids were imaged and analyzed by edge-detection/thresholding method on ImageJ software. A significant change between empty vector (EV) and AKR1B1 overexpressing cells was observed with the area of the spheroids. Two independent biological replicates were used for statistical analysis. N ≈12. Significance was determined by One-way ANOVA. *p<0.05, **p<0.01.*

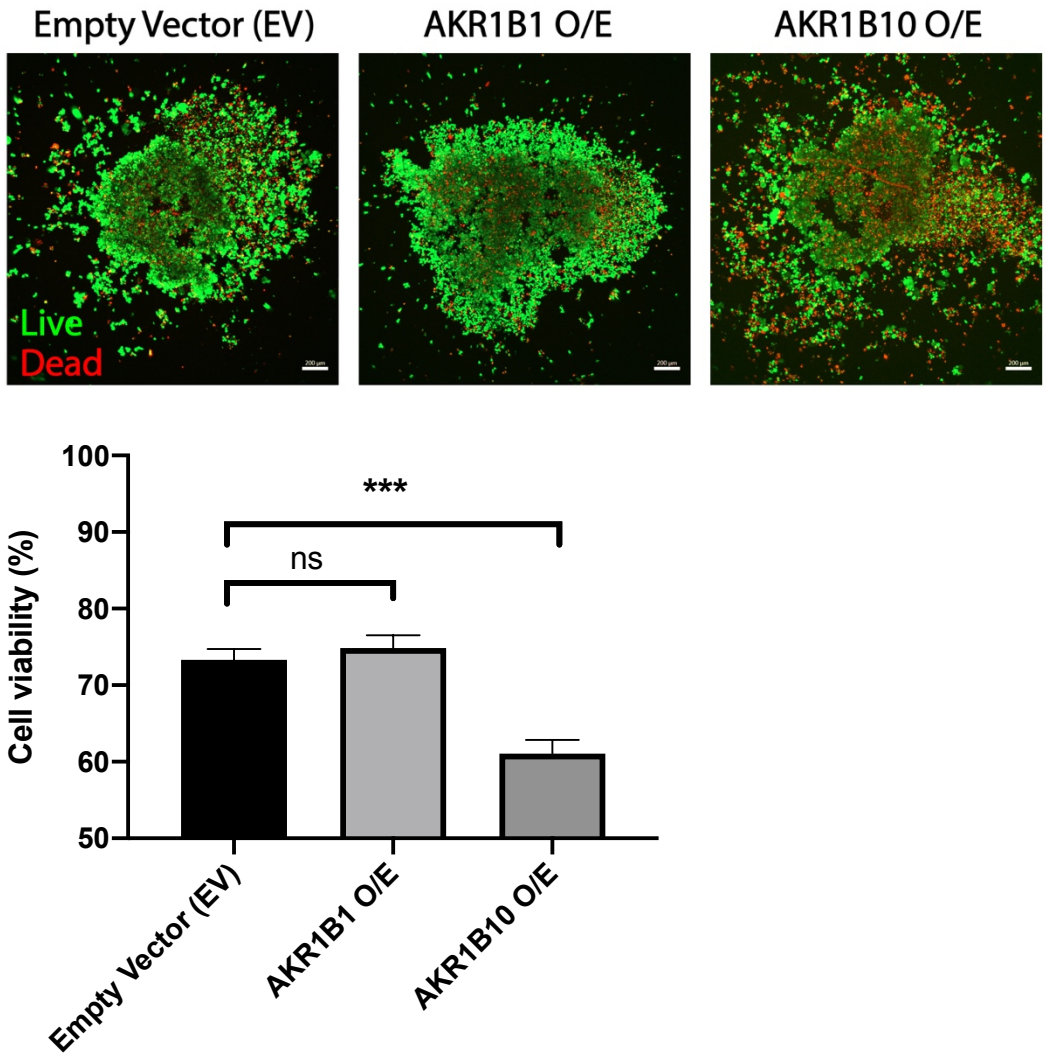

Figure 13. *Live-dead staining assay of AKR1B1 and AKR1B10 overexpressing cells in 3D cell culture*

SW480 empty vector (EV), AKR1B1 overexpressing, and AKR1B10 overexpressing cells were seeded to 96 well ULA plates at 10,000 cells/well density and cultured for 5 days to promote spheroid formation. After 5 days, spheroids were stained with

*Calcein (green dots, live-cells) and Ethidium homodimer (red dots, dead-cells), imaged, then analyzed by edge-detection/thresholding method on ImageJ software. N ≈6. Significance was determined by One-way ANOVA. *p<0.05, **p<0.01, ***p<0.0001.*

In order to investigate the viability of the cells in the core of the spheroids, live-dead staining assay was carried out for SW480 empty vector (EV) and AKR1B1 or AKR1B10 overexpressing cells (Figure 13). Data obtained from this assay showed us that there was a significant difference between empty vector (EV) and AKR1B10 overexpressing cells in the case of core viability, while AKR1B1 overexpressing cells showed a similar core viability profile with empty vector (EV).

3.3 Effect of AKR1B1 and AKR1B10 overexpression on cellular motility in SW480 cells

We next determined whether the overexpression of AKR1B1 or AKR1B10 overexpression affected the motility of SW480 cells. For this, a wound-healing assay was performed (Figure 14). Overexpression of AKR1B1 increased the cellular motility significantly compared to the Empty Vector (EV) control cells in 72 hours. Additionally, AKR1B10 overexpression resulted in a significant loss of motility when compared to the AKR1B1 overexpressing cells, especially at the 48h and 72h time points. Of note, the cells were treated with mitomycin C during the wound healing assay to ensure that the wound closure did not result from the proliferation of the cells.

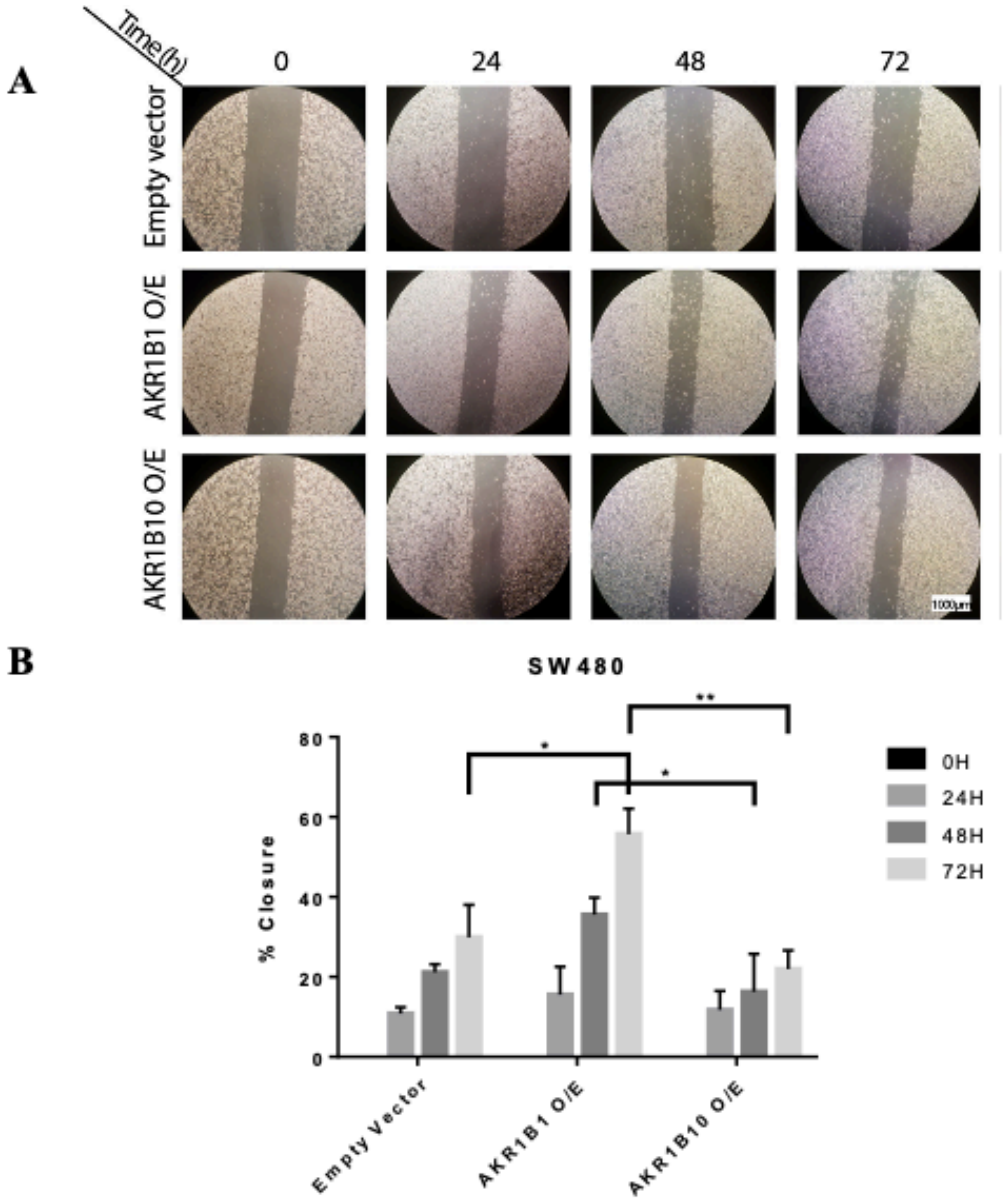

Figure 14. *Effects of AKR1B1 and AKR1B10 overexpression on cell motility using the wound healing assay*

*SW480 empty vector (EV), AKR1B1, and AKR1B10 overexpressing cells were seeded to a 6 well plate at a density of 1,000,000 cells/well. Cells were cultured to 95% confluency, and scratch wounds were generated in each well by using 100 µl pipette tips. The cell medium was replaced with fresh complete medium containing 0.5 µM Mitomycin C and images of the wells were taken every 24 hours. The obtained images were analyzed by the edge-detection/thresholding method on ImageJ software. Two independent biological replicates were used for statistical analysis. Significance was determined by Two-way ANOVA. *p<0.05, **p<0.01.*

3.4 Effect of AKR1B1 and AKR1B10 overexpression on cell cycle in SW480 cells

To assess the effects of AKR1B1 or AKR1B10 overexpression on the cell cycle of SW480 cells, flow cytometry analysis with PI staining (Figure 15 & Figure 16) was carried out. Two different sets of cells were used for these assays; synchronized and freely cycling cells, respectively. Both sets of cells were seeded at the same time, and FBS starved for synchronizing their cell cycle at the G1 phase. After 16h of starvation, one set was collected and fixed, then the remaining set was released for free cycling by changing the medium with complete medium and collected after 8h. Half of the cells collected from both sets were used for flow cytometry experiments, and the other half were used for western blotting. In the free cycling set of cells, significant differences were observed between Empty Vector (EV) and AKR1B10 overexpressing cells at the G1 and G2M phases of the cell cycle by both flow cytometry analysis and western blotting experiment.

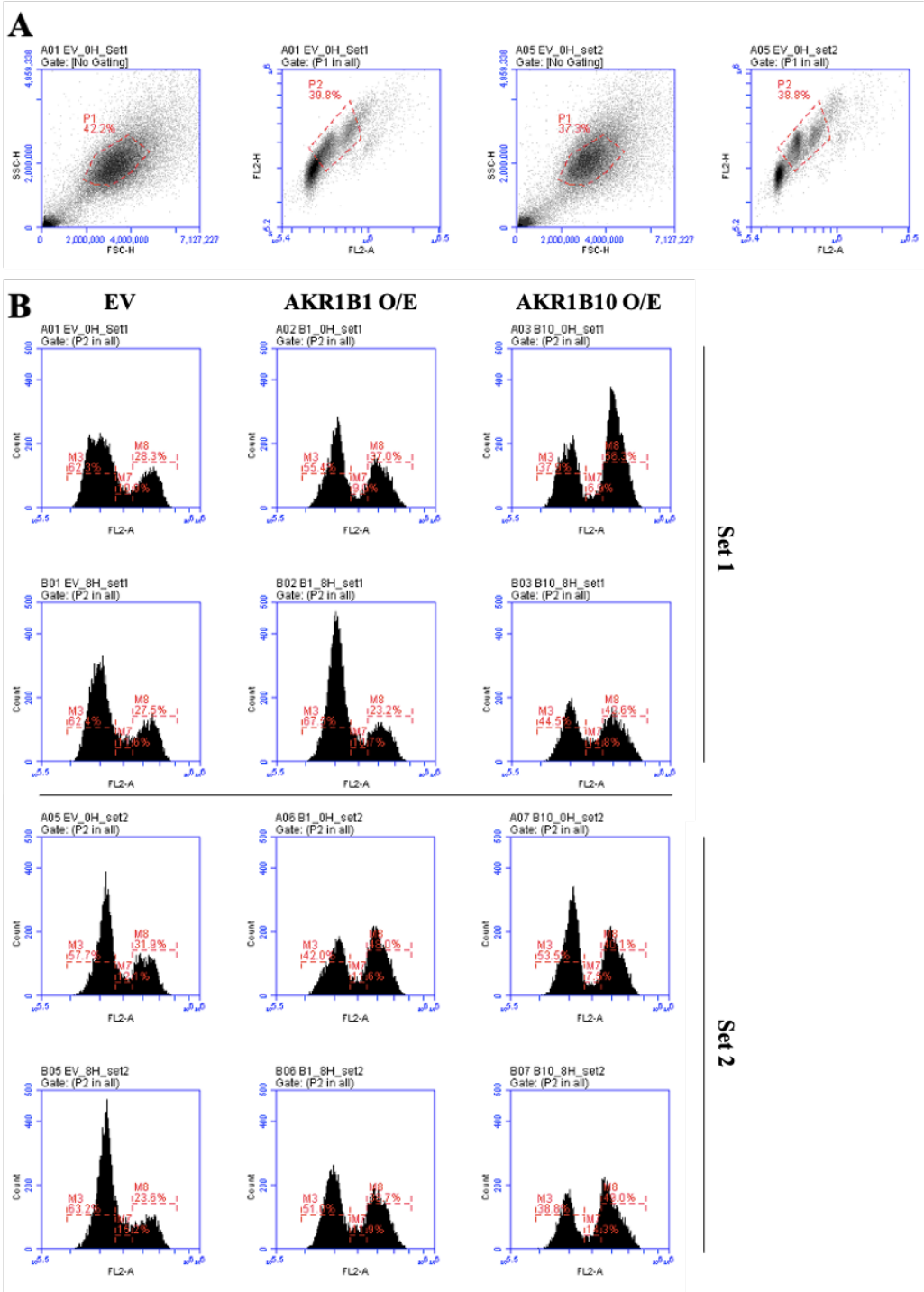

Figure 15. *Effects of AKR1B1 and AKR1B10 overexpression on cell cycle progression using the flow cytometry*

SW480 empty vector (EV), AKR1B1, and AKR1B10 overexpressing cells were seeded to a 6 well plate at a density of 500,000 cells/well. Starved and free cycled groups were collected and stained with the PI solution in order to determine their

*cell cycle status using flow cytometry. **(A)** Cell populations were gated in order to eliminate debris and clumped cells, leaving only alive and singlet cells for analysis. **(B)** Percent distribution of the cell cycle status of both groups in FL-2 channel. Percentages show G1, S, and G2M phases of cell cycle respectively in each histogram. Two independent biological replicates were illustrated in histograms as set 1 and set 2.*

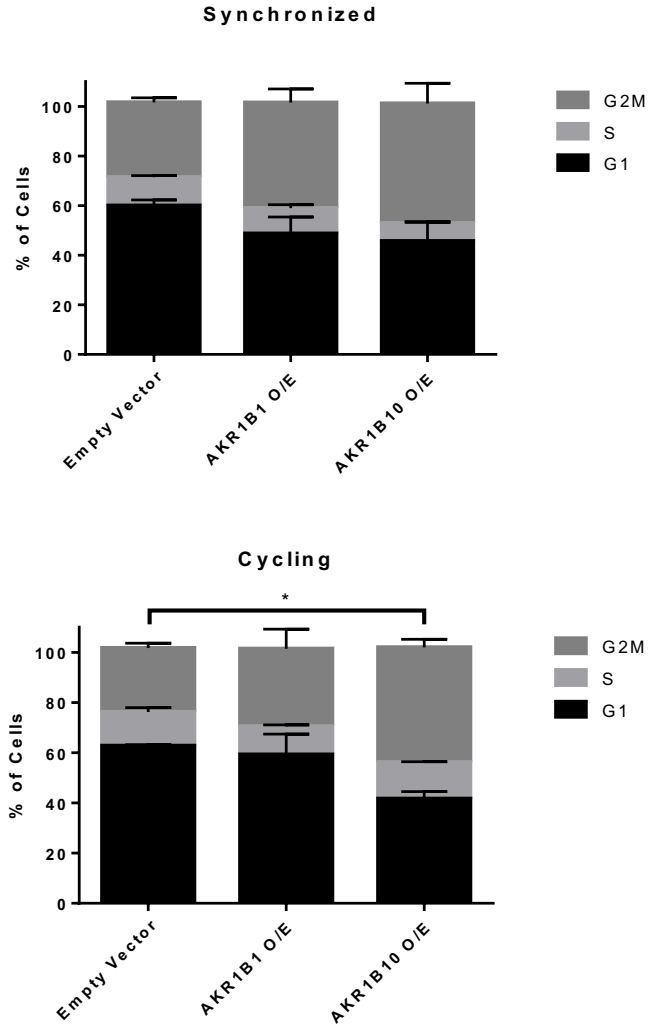

Figure 16. *Cell cycle distribution of starved and free cycling cells*

SW480 empty vector (EV), AKR1B1, and AKR1B10 overexpressing cells were analyzed for their cell cycle status using flow cytometry. No significant change was observed in the synchronized cells. In cycling cells, significant changes were observed between empty vector (EV) and AKR1B10 overexpressing cells in G1 and

*G2M phases. Two independent biological replicates were used for statistical analysis. Significance was determined by Two-way ANOVA. *p<0.05, **p<0.01.*

To confirm the significantly higher percentage of AKR1B10 overexpressing cells at the G2M phase, we evaluated the expression of cyclin B1 (Figure 17). This cyclin is associated with G2-M transition, and its loss is suggestive of cells that are arrested at the S phase (Ling *et al.,* 1998). We did not observe any expression of cyclin B1 in the G1/S synchronized cells as cyclin B1 is not expected to be expressed at that stage of the cell cycle. We observed in two independent sets of proteins a nearly complete loss of cyclin B1 in the AKR1B10 overexpressing cells compared to the EV or AKR1B1 overexpressing cells. This suggests that the AKR1B10 overexpressing cells are slower in their cell cycle progression compared to the control or AKR1B1 expressing cells, which expressed higher amounts of cyclin B1 and were likely to be at the G2M phase already. HCT-116 cells treated with Actinomycin D, which arrests cells at, G2M was used as a positive control.

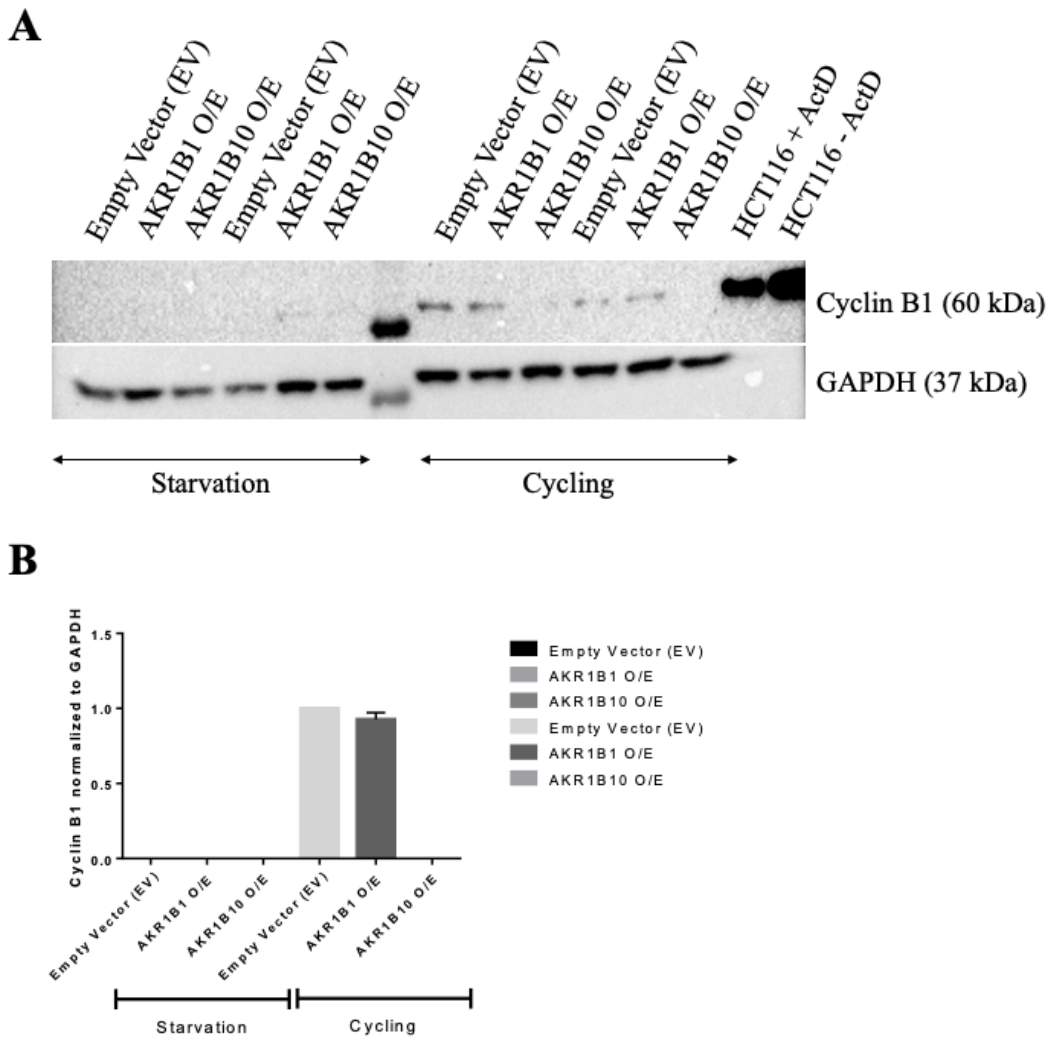

Figure 17. *Effects of AKR1B1 and AKR1B10 overexpression on cell cycle progression by western blotting*

Proteins collected from SW480 empty vector (EV), AKR1B,1, and AKR1B10 overexpressing cells were western blotted to check their Cyclin B1 levels. ***(A)*** *All sets of cells (starvation & cycling) were starved for 16h with 0% FBS containing medium for synchronization. Then medium of one set was replaced with complete-medium in order to release cells for free cycling for 8h. HCT116 Actinomycin D (ActD) treated and non-treated samples were also added to the western blot as G2M arrest controls.* ***(B)*** *Quantification of Cyclin B1 antibody blotting normalized to GAPDH. GAPDH antibody was used as a loading control. Two independent biological replicates were assessed.*

3.5 Effect of AKR1B1 and AKR1B10 overexpression on Pentose Phosphate Pathway in SW480 cells

PPP is a pathway that can utilize glucose-6-phosphate generated from glycolysis for the synthesis of ribose-6-phosphate. The latter is utilized for the synthesis of nucleotides. NADPH is generated in the pathway, which can be utilized by the glutathione antioxidant system to reduce oxidative stress in cells. The PPP is, therefore, an essential pathway for cancer cells to survive and is known to be hyper-activated in different cancer types (Ge *et al.,* 2020). AKR1B1 and AKR1B10 are known to utilize reducing electrons from NADPH, and previous in silico data from our lab (Sheraj, I. and Banerjee, S., unpublished data) suggest that the expression of AKRs was strongly positively correlated with the expression of PPP genes. Therefore, to investigate the effect of AKR1B1 and AKR1B10 overexpression on PPP, qRT-PCR and western blotting assays were conducted to determine the expression of G6PD. G6PD is an important target to investigate since it is a rate-limiting enzyme of PPP, and its activity is closely regulated. qRT-PCR assay showed a significant decrease in the mRNA expression of G6PD in AKR1B10 overexpressed cells compared to empty vector (EV) control SW480 cells, while an increase in expression was observed in the AKR1B1 overexpressing cells (Figure 18).

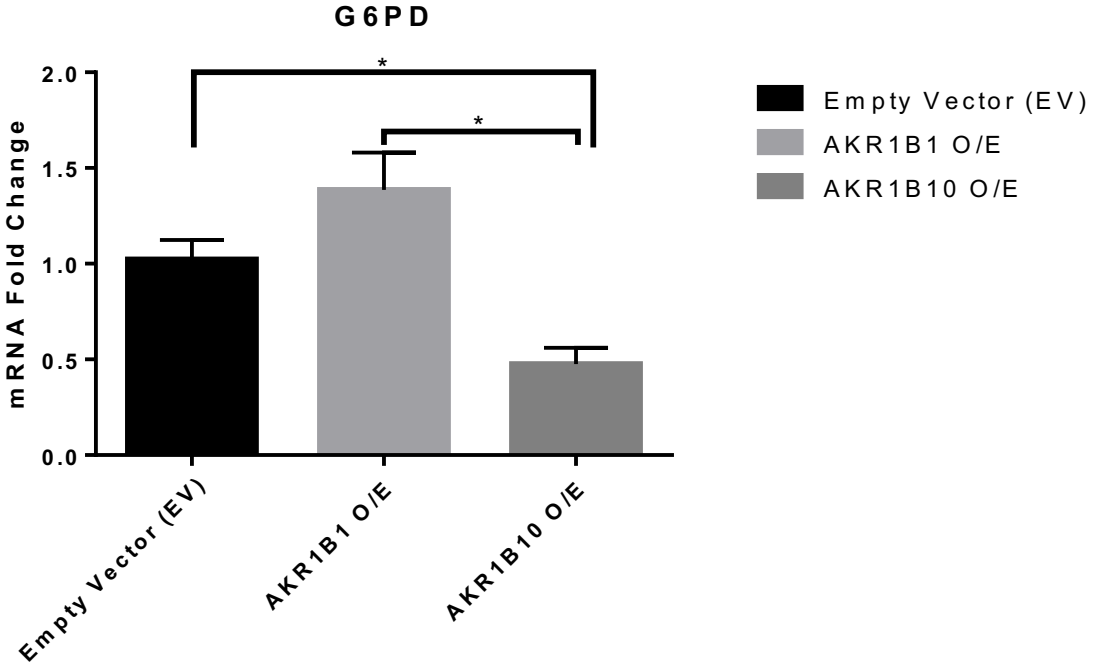

Figure 18. *Effects of AKR1B1 and AKR1B10 overexpression on G6PD transcription by qRT-PCR*

*To compare the transcriptional levels of the G6PD gene in empty vector (EV), AKR1B1, and AKR1B10 overexpressing cells, qRT-PCR was conducted. 1 µg of sample cDNA was used in 1:10 dilution for each reaction with 3 internal replicates. Reactions were conducted in 40 cycles. B-actin was used as an internal control for qRT-PCR. Obtained data were normalized to B-actin and analyzed by using the Pfaffl method (Pfaffl, 2001). Two independent biological replicates were used for statistical analysis. Significance was determined by One-way ANOVA. *p<0.05, **p<0.01.*

We next determined the protein expression of G6PD. For this, we used two different protein samples. In one set, we used overnight serum-starved cells, while in the other, we used cells grown in complete medium. This setup was used as we hypothesized that low nutrient availability might exacerbate the regulation of G6PD expression and its activity. We observed that in serum-starved cells, the expression of G6PD was increased in the AKR1B1 expressing cells while the same in AKR1B10 overexpressing cells remained the same as the controls (Figure 19A). The protein

expression of G6PD was in the serum replete cells was slightly lower in both AKR1B1 and AKR1B10 overexpressing cells (Figure 19B).

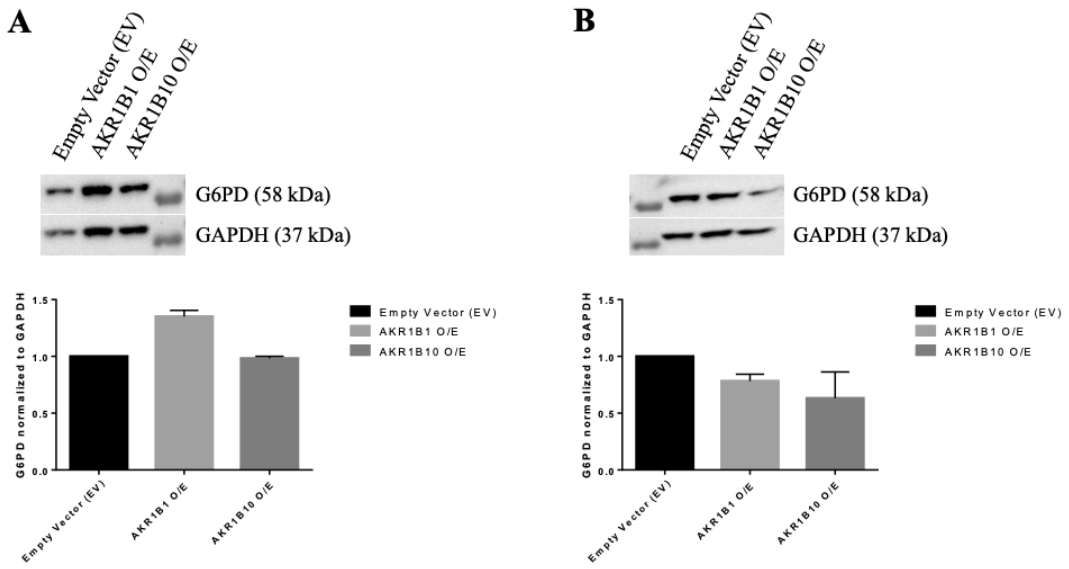

Figure 19. *Effects of AKR1B1 and AKR1B10 overexpression on G6PD protein levels by western blotting*

Proteins collected from SW480 empty vector (EV), AKR1B1, and AKR1B10 overexpressing cells were evaluated for G6PD protein expression by western blot ***(A)*** *Protein expression of G6PD in FBS starved SW480 cells.* ***(B)*** *Protein expression of G6PD in cells grown in complete medium. The band intensity of G6PD was normalized to the band intensity of GAPDH (loading control). Two independent biological replicates were assessed.*

CHAPTER 4

DISCUSSION

There are many structurally related enzymes of common ancestry that catalyze redox transformations involved in biosynthesis, intermediate metabolism, and detoxification in the Aldo-Keto Reductase (AKR) superfamily. Glucose, steroids, glycosylation end products, lipid peroxidation products, and environmental pollutants represent the substrates of these enzymes. These proteins have $(\beta\ \alpha)_8$ or Triose-phosphate isomerase (TIM)-barrel motif that is a compact but adaptable scaffolding with structural variations that can bind to a range of carbonyl substrates that are chemically diverse (Jez *et al.,* 1997). Using NADPH as the cofactor, most AKRs catalyze simple oxidation-reduction reactions. The main task of these enzymes is to catalyze the reduction of aldehyde and ketone substrates into their primary and secondary alcohol products (Penning and Drury, 2007). AKR's role in metabolism is relatively simple yet very crucial for most pathways to work properly in the human body. Therefore, any direct or indirect deregulation of this family of enzymes has been implicated in diabetes (Wallner *et al.,* 2001) and carcinogenesis (Penning and Byrns, 2009; Ramana, 2011).

In this thesis study, we aimed to investigate the functional effects of AKR overexpression on CRC. The reason for choosing AKR enzymes as the topic of interest comes from previous *in-silico* analysis conducted on CRC patient data in our lab. Using publicly available AKR1B1 and AKR1B10 expression data in samples of patients with colon cancer using microarray data as well as the TCGA portal, we observed that the expression of AKR1B10 in cancer samples was significantly lower compared to normal samples, whereas the expression of AKR1B1 between cancer and normal was similar (Taşkoparan *et al.,* 2017). A number of functional changes upon silencing of endogenously expressed AKR1B1 in CRC cell lines were observed, such as slowing down of cell cycle, slower motility, and lower

inflammation. All of these phenotypes were supported by expression and gene set enrichment analyses carried out *in silico* (Taşkoparan *et al.,* 2017; Demirkol *et al*., 2020). The effect of AKR1B10 on cancer is highly context dependent. While we and others have observed a tumor suppressive role of AKR1B10 in CRC (Ohashi *et al.,* 2013; Yao *et al.,* 2020), a previous study has reported that silencing of AKR1B10 in the CRC cell line HCT-8 could induce inhibition in cell growth, suppression of DNA synthesis and reduction of clonogenic growth capacity. Silencing of this gene also increased the sensitivity of the cells to reactive carbonyls, crotonaldehyde and acrolein (Yan *et al.,* 2007). In a different study, when grown on soft substrates for 20 days, HCT-8 cells were found to transition from an epithelial (E) phenotype to an unusual, more rounded (R) highly metastatic phenotype. The cells of 'R' expressed significantly higher amounts of AKR1B10 than the cells of 'E' (Tang *et al.,* 2014). On the other hand, the proliferation rate was observed significantly higher for AKR1B10 knockdown HT29 cells and was inhibited by that of AKR1B10 over-expressing HCT116 cells. The AKR1B10-knockdown cells also displayed improved colony-formation potential consistent with this, which was markedly suppressed in the AKR1B10-over-expressing cells (Yao *et al.,* 2020). Thus, in epithelial type CRC cells that predominate in most of the models used to date, AKR1B10 expression is likely to be low. While these studies shed light on many important aspects about the correlation between expression of the enzymes and progression of CRC, it provided a basis to determine whether overexpression of AKR1B1 and AKR1B10 in different CRC cell models would enable us to mechanistically determine the signaling pathways involved in the functional alterations observed.

Therefore, as a part of a COST Action (CA17118), we designed a study that can evaluate the role of AKR1B1 and AKR1B10 on cellular energetics and EMT. Two cell lines were used as a part of the study, RKO, and SW480. Neither cell line endogenously expresses AKR1B1 or AKR1B10 (Taşkoparan *et al.,* 2017), but their energy metabolisms are highly diverse as ATCC recommends RKO cells to be cultured in glucose-containing medium and SW480 cells to be cultured in galactose containing medium. The use of galactose as the source of carbohydrates entails a

preferential use of the TCA cycle and OXPHOS rather than oxidative glycolysis (Shiratori *et al.,* 2019). Cells first need to convert galactose to glucose-1-phosphate (G-1P) via the Leloir Pathway; only then can G-1P enter into glycolysis. Galactose can also be converted to UDP-glucose via the Leloir Pathway, as an alternative pathways and this UDP-glucose has the potential to enter the PPP (Tang *et al.,* 2016). GLUT1, GLUT2 and GLUT8 are all capable of transport galactose into cells (Mueckler & Thorens, 2014) but the primary transporter of galactose is SGLT1 (Levin, 1994). This difference opens up a whole new approach to the experiments as AKRs are known to utilize glucose as a substrate. My thesis study was carried out with SW480 cells, and the content of this thesis study must be evaluated in the context of the presence of galactose.

I first evaluated whether AKR1B1 or AKR1B10 overexpression altered the proliferative capacity of SW480 cells. Three different assays were carried out: MTT, colony formation, and spheroid formation assays. MTT assay was conducted in order to investigate whether the overexpression of AKR1B1 or AKR1B10 affected the proliferative and/or metabolic capacity of the cells. At the end of 72h, no significant change in proliferation was observed between EV and AKR1B1 or AKR1B10 overexpressed cells (Figure 10). As the SW480 cells utilize OXPHOS, which is a slower source of ATP compared to aerobic glycolysis (Pfeiffer *et al.,* 2001), we hypothesized that a longer-term colony formation assay might be more informative. Indeed, we observed a significant decrease in the colony formation ability of AKR1B10 overexpressing cells compared to the EV (Figure 11). Previous *in silico* data from our lab suggests that high AKR1B10 expression was linked with a good prognosis in CRC (Demirkol *et al.,* 2020). The reduction in colony formation with AKR1B10 overexpression suggests a weaker proliferative ability in these cells when examined over several population doublings providing a functional basis for the good prognosis observed. Moreover, high AKR1B10 was shown to decrease glycolytic capacity in metastatic breast cancer (Weverwijk *et al.,* 2019), suggesting that enhanced OXPHOS may be the reason for the slower proliferation in these cells.

A modest increase in colony formation ability was observed in AKR1B1 overexpressed cells. *In silico* data from our lab has shown that $AKR1B1^{HIGH}/AKR1B10^{LOW}$ CRC tumor samples were primarily classified as Consensus Molecular Subtype 4 (CMS4) with predominantly mesenchymal characteristics (Demirkol *et al.,* 2020). AKR1B1 enzyme was also linked with EMT in several other cancer types, such as basal-like breast cancer (Wu *et al.,* 2017). Mesenchymal cells, by definition, are poorly proliferative but can survive in conditions of poor cell-cell adherence and are more motile than epithelial cells. The clonogenic assay also reflects the ability of cells to overcome contact inhibition, and the slightly enhanced colony formation ability of the AKR1B1 overexpressing cells may be reflective of cells that are further resistant to contact inhibition.

To better evaluate this, the cells were grown in 3D cell culture conditions using a spheroid formation assay in ultra-low attachment plates. The proliferative capacities of the cells were assessed by the measured area of the spheroids individually. In theory, spheroids with the bigger area are suggestive of a higher rate of proliferation. However, a larger spheroid may also mean that lower cell-cell adhesion and spread of the cells in 3D. So, while interpreting the results, in addition to area measurements, the tightness of the spheroids should also be considered. We observed significantly larger spheroids with AKR1B1 overexpressing cells compared to EV or AKR1B10 overexpressing cells. Additionally, unlike EV and AKR1B10 overexpressed spheroids, AKR1B1 overexpressed spheroids were a lot looser. For a deeper understanding of the behaviour of these cells in 3D culture conditions, live-dead cell staining viability assay was also conducted on the spheroids. According to the data obtained from this assay, we can see that there is a significant difference between the cell viability of AKR1B10 overexpressing cells compared to EV (Figure 13). Hypoxia and necrosis are important tumor phenomena that may occur in the culture of an in vitro spheroid. Generally, in terms of the supply of oxygen and nutrients, a tumor spheroid has three regions, namely necrotic, hypoxic or quiescent and proliferating zones. The shortage of oxygen and nutrients contributed to cell death due to starvation in the necrotic zone (Barisam *et al.,* 2018). We think that AKR1B10

overexpression sensitizes these cells to hypoxia and nutrient starvation significantly more than AKR1B1 overexpression. This claim can also be supported qualitatively by the confocal images shown in Figure 13 that upon addition of the dyes on the spheroids, due to the physical disruption of the media that spheroids cultured in, AKR1B10 overexpressing samples were burst due to the extensive cell death caused by hypoxia and nutrient starvation, since other samples stays intact. These data further support our observations that AKR1B1 expression leads to weaker cell-cell adhesion and a stronger mesenchymal phenotype, however AKR1B10 overexpression sensitizes these cells to hypoxia and nutrient starvation.

To further support the association of AKR expression on EMT, we determined cellular motility using the scratch wound healing assay in SW480 cells. We observed that AKR1B1 overexpressing SW480 cells had higher motility reflected by a faster closure of the wound compared to EV and AKR1B10 overexpressing cells (Figure 14). The faster wound closure was not due to enhanced proliferation as the cells were treated with mitomycin C that inhibits proliferation. These experiments show overall that AKR1B1 overexpression might positively upregulate EMT and increase mesenchymal character in SW480 cells.

To understand why the AKR1B10 overexpressing cells form fewer colonies in the clonogenic assay, we determined the effect of AKR1B1 or AKR1B10 overexpression on cell cycle progression with PI staining as well as western blot (Figures 16 and 17). We observed that when the cells were released after synchronization, a greater proportion of AKR1B10 overexpressing cells were at the S and G2M phase compared to the EV or AKR1B1 overexpressing cells. SW480 cells have a population doubling time of 24h (Cowley *et al.,* 2014), suggesting that AKR1B10 overexpression may slow down the cell cycle progression such that the major population of the AKR1B1 cells had already passed the G2M phase and entering G1 phase again, but the major population observed in the AKR1B10 cells were stuck in the G2M phase and the only transition observed in these cells were from the G1 to the S phase. This evaluation of the PI staining data is supported by the protein levels of cyclin B1. Cyclin B1's function is to induce the transition of

cells from the G2 phase to the M phase (Jang *et al.,* 2016). It is likely that the high levels of cyclin B1 in EV and AKR1B1 overexpressing cell lines was because these cells were already passed from the G2 to the M phase, while the AKR1B10 overexpressing cells were still at S phase and therefore had significantly less cyclin B1. The high percentage of cells at the S phase in the cycling /released AKR1B10 expressing cells compared to AKR1B1 or control cells is also a testament to our interpretation of the data.

One of the primary hypotheses for our study was to determine whether AKR1B1 or AKR1B10 can affect cellular energetics. Given the fact that AKR enzymes utilize NADPH and PPP is the primary source of NADPH in the cytosol, we investigated the expression of G6PD, the rate-limiting enzyme of PPP that converts glucose-6 phosphate (from glycolysis) to 6-phosphogluconolactone with the generation of NADPH. We observed a significant decrease in the mRNA expression of G6PD in AKR1B10 overexpressing cells (Figure 18). A decrease in protein levels was also observed in the AKR1B10 overexpressing cells (Figure 19B); however, variations were seen between replicates. We then determined the G6PD protein levels in cells that were starved of serum for 16h, we observed that starved AKR1B1 overexpressing cells showed a higher expression of G6PD compared to EV and AKR1B10 cells (Figure 19A). Although enzymatic activity cannot be determined solely on the basis of expression, our data suggest that the upregulation of G6PD in the starved AKR1B1 overexpressing cells may help the cells cope with nutrient stress. It is well known that serum deprivation leads to the production of ROS (Lee et al., 2010); therefore, the upregulation of G6PD in AKR1B1 overexpressing cells may lead to any available glucose-6-phosphate being preferentially shunted to the PPP, generating more NADPH, which can then be used to mitigate oxidative stress (Kuehne *et al.,* 2013). We can speculate that this helps the AKR1B1 cells to proceed through the cell cycle effectively and continue proliferating. For AKR1B10 cells, considering the lower viability of these cells in 3D culture and the slower progression through the cell cycle, it can be suggested that overexpression of AKR1B10 enhances the sensitivity of these cells to nutrient starvation. One possible explanation

for this phenomenon could be via the effect of AKR1B10 on retinoid metabolism. The end product of retinoid metabolism is retinoic acid. Retinoic acid receptor (RAR) is a nuclear receptor that is activated by both all-*trans* retinoic acid and 9-*cis* retinoic acid while RXR is activated by 9-*cis* retinoic acid, but not the *trans* form (Allenby *et al.,* 1993). RAR can heterodimerize with RXR and bind to consensus sequences called RARE to initiate expression of genes important in differentiation, development and apoptosis. AKR1B10, unlike AKR1B1, is an efficient retinaldehyde reductase with a high k_{cat} value (Ruiz *et al.,* 2012). When AKR1B10 is overexpressed in a cell, it can enhance the reduction of retinaldehyde to retinol rather than the oxidation of retinaldehyle to retinoic acid. Reduced availability of retinoic acid can result in decreased transcriptional activity of the RAR-RXR heterodimer. RXR is known to affect glucose metabolism (Rhee & Plutzky, 2012). RXRγ overexpression in mice showed greater glucose disposal compared to control mice, and insulin-independent increase in GLUT1 expression was seen in the skeletal muscle of mice overexpressing RXRγ (Sugita *et al.,* 2011). It is feasible to speculate that reduced activation of RAR-RXR in AKR1B10 overexpressing cells may reduce the expression of GLUT1 thereby decreasing the entry of glucose and galactose into cells that may eventually downregulate the expression of G6PD.

CHAPTER 5

CONCLUSION

Aldo-keto reductases (AKRs) are a superfamily of enzymes that are involved in phase 1 metabolism of carbonyl substrates such as sugars, lipid aldehydes, keto-steroids, and keto-prostaglandins are (Chang and Petrash, 2018). Given the variety of biological aldehydes that can potentially act as substrates for these enzymes, the transformation and detoxification of aldehydes and ketones formed endogenously during metabolism or found in the environment as nutrients, food, drugs, or toxins are likely to be the most important function of the AKR superfamily (Bachur *et al*., 1976). The role of AKRs in metabolism is relatively simple but critical for most pathways in the human body to function properly. Therefore, any direct or indirect deregulation of these enzyme families may imply a disorder such as diabetes (Wallner *et al.,* 2001) and carcinogenesis (Penning and Byrns, 2009; Ramana, 2011).

We hypothesized that overexpression of AKR1B1 or AKR1B10 might have significant effects on energy metabolism and EMT in the CRC cell line SW480.

Our primary findings have been listed below.

1. AKR1B1 or AKR1B10 overexpression did not lead to any alteration in cell proliferation in the short term (24-72h); however, a long-term clonogenic assay showed significantly fewer clones in the AKR1B10 overexpressing cells. These data support our previous *in silico* finding that high AKR1B10 expression in CRC patients leads to better survival compared to patients with high AKR1B1 expressing tumors.
2. AKR1B1 overexpressing cells formed significantly bigger but looser spheroids when grown in 3D in ultra-low attachment plates suggesting the

presence of weaker cell-cell adhesions. This was supported by increased motility in a 2D scratch wound healing assay. These data also support our previous finding that AKR1B1 expression was strongly positively correlated with mesenchymal markers in fresh frozen tissue samples from CRC patients. Live-dead cell viability assay on spheroids grown in 3D also showed an increased necrotic core on AKR1B10 cells, suggesting that AKR1B10 expression sensitizes these cells for nutrient restriction and hypoxia.

3. AKR1B10 (but not AKR1B1) overexpressing cells were found to progress more slowly through the cell cycle compared to AKR1B1 or control EV cells. This may have resulted in the reduced clonogenic capacity of these cells.
4. In starved AKR1B1 overexpressing cells, G6PD expression was found to be higher than the control cells. We speculate that AKR1B1 overexpressing cells may survive the oxidative stress that results from serum starvation by upregulating G6PD. This would also lead to the generation of NADPH that can feed into the glutathione antioxidant system, thereby mitigating oxidative stress.

Several unanswered questions will be addressed in future studies:

1. Further elaboration of the migratory and invasive capacity of these cells, especially under conditions of serum withdrawal.

2. Better elaboration of the role of AKRs on the NADPH/NADP ratio in cells. There are several pathways that are known to contribute towards the NADPH pool in the cytosol, and it is unclear whether these pathways are affected when AKRs are overexpressed. However, an evaluation of the NADPH/NADP ratio in serum-starved versus unstarved cells would provide us clues on the activity of NADPH generating and utilizing pathways. In the same context, the GSSG/GSH levels and ROS levels will also be evaluated in serum-starved and unstarved SW480 cells expressing AKR1B1 or AKR1B10.

Overall, my data has provided indications of activation signaling pathways related to metabolism that may affect the metastatic and invasive capacity of colon cancer cells. Recent studies indicate that metabolic intermediates are not a by-product of growth factor signaling; instead, they may actually directly activate mitogenic pathways (Xu *et al .,* 2021). Our data suggest that the expression of AKRs can also affect several different hallmarks of cancer, lending credence to the inclusion of deregulated metabolism as an emerging hallmark (Hanahan and Weinberg, 2011). Our future efforts will be directed at better elucidating the crosstalk between whether enzymatic pathways such as AKRs or PPP that utilize/generate metabolic intermediates such as NADPH and whether this cross-talk can address the functional changes observed in the AKR high/low expressing cells.

REFERENCES

Abe, A., Miyanohara, A., & Friedmann, T. (1998). Polybrene increases the efficiency of gene transfer by lipofection. *Gene Therapy* (Vol. 5). Retrieved from http://www.stockton-press.co.uk/gt

Ahmed, D., Eide, P. W., Eilertsen, I. A., Danielsen, S. A., Eknæs, M., Hektoen, M., … Lothe, R. A. (2013). Epigenetic and genetic features of 24 colon cancer cell lines. *Oncogenesis*, *2*(9). https://doi.org/10.1038/oncsis.2013.35

Allenby, G., Bocquel, M. T., Saunders, M., Kazmer, S., Speck, J., Rosenberger, M., … Levin, A. A. (1993). Retinoic acid receptors and retinoid X receptors: Interactions with endogenous retinoic acids. *Proceedings of the National Academy of Sciences of the United States of America*, *90*(1), 30–34. https://doi.org/10.1073/pnas.90.1.30

Bachur, N. R. (1976). Cytoplasmic aldo-keto reductases: A class of drug metabolizing enzymes. *Science*, *193*(4253), 595–597. https://doi.org/10.1126/science.959821

Barisam, M., Saidi, M. S., Kashaninejad, N., & Nguyen, N. T. (2018). Prediction of necrotic core and hypoxic zone of multicellular spheroids in a microbioreactor with a U-shaped barrier. *Micromachines*, *9*(3). https://doi.org/10.3390/mi9030094

Barnes, E. M. E., Xu, Y., Benito, A., Herendi, L., Siskos, A. P., Aboagye, E. O., … Keun, H. C. (2020). Lactic acidosis induces resistance to the pan-Akt inhibitor uprosertib in colon cancer cells. *British Journal of Cancer*, *122*(9), 1298–1308. https://doi.org/10.1038/s41416-020-0777-y

Barski, O. A., Tipparaju, S. M., & Bhatnagar, A. (2008, October). The aldo-keto reductase superfamily and its role in drug metabolism and detoxification. *Drug Metabolism Reviews*. NIH Public Access. https://doi.org/10.1080/03602530802431439

Bhowmick, N. A., Neilson, E. G., & Moses, H. L. (2004, November 18). Stromal fibroblasts in cancer initiation and progression. *Nature*. NIH Public Access. https://doi.org/10.1038/nature03096

Bokun, R., Bakotin, J., & Milasinović, D. (1987). Semiquantitative cytochemical estimation of glucose-6-phosphate dehydrogenase activity in benign diseases and carcinoma of the breast. *Acta Cytol*. PMID: 3035846.

Bril, V., & Buchanan, R. A. (2006). Long-term effects of ranirestat (AS-3201) on peripheral nerve function in patients with diabetic sensorimotor polyneuropathy. *Diabetes Care*, *29*(1), 68–72. https://doi.org/10.2337/diacare.29.01.06.dc05-1447

Brisson, L., Bański, P., Sboarina, M., Dethier, C., Danhier, P., Fontenille, M. J., … Sonveaux, P. (2016). Lactate Dehydrogenase B Controls Lysosome Activity and Autophagy in Cancer. *Cancer Cell*, *30*(3), 418–431. https://doi.org/10.1016/j.ccell.2016.08.005

Cabezas, H., Raposo, R. R., & Meléndez-Hevia, E. (1999). Activity and metabolic roles of the pentose phosphate cycle in several rat tissues. *Molecular and Cellular Biochemistry*, *201*(1–2), 57–63. https://doi.org/10.1023/a:1007042531454

Cao, D., Fan, S. T., & Chung, S. S. M. (1998). Identification and characterization of a novel human aldose reductase- like gene. *Journal of Biological Chemistry*, *273*(19), 11429–11435. https://doi.org/10.1074/jbc.273.19.11429

Cao, H., Xu, E., Liu, H., Wan, L., & Lai, M. (2015, August 1). Epithelial-mesenchymal transition in colorectal cancer metastasis: A system review. *Pathology Research and Practice*. Elsevier GmbH. https://doi.org/10.1016/j.prp.2015.05.010

Ceccarelli, J., Delfino, L., Zappia, E., Castellani, P., Borghi, M., Ferrini, S., … Rubartelli, A. (2008). The redox state of the lung cancer microenvironment depends on the levels of thioredoxin expressed by tumor cells and affects tumor progression and response to prooxidants. *International Journal of Cancer*, *123*(8), 1770–1778. https://doi.org/10.1002/ijc.23709

Cha, M. K., Suh, K. H., & Kim, I. H. (2009). Overexpression of peroxiredoxin i and thioredoxin1 in human breast carcinoma. *Journal of Experimental and Clinical Cancer Research*, *28*(1). https://doi.org/10.1186/1756-9966-28-93

Chang, K. C., & Petrash, J. M. (2018). Aldo-keto reductases: Multifunctional proteins as therapeutic targets in diabetes and inflammatory disease. In *Advances in Experimental Medicine and Biology* (Vol. 1032, pp. 173–202). Springer New York LLC. https://doi.org/10.1007/978-3-319-98788-0_13

Cheng, N., Chytil, A., Shyr, Y., Joly, A., & Moses, H. L. (2008). Transforming growth factor-β signaling-deficient fibroblasts enhance hepatocyte growth factor signaling in mammary carcinoma cells to promote scattering and invasion. *Molecular Cancer Research*, *6*(10), 1521–1533. https://doi.org/10.1158/1541-7786.MCR-07-2203

Cho, E. S., Cha, Y. H., Kim, H. S., Kim, N. H., & Yook, J. I. (2018, January 1). The pentose phosphate pathway as a potential target for cancer therapy. *Biomolecules and Therapeutics*. Korean Society of Applied Pharmacology. https://doi.org/10.4062/biomolther.2017.179

Cook, A. D., Single, R., & McCahill, L. E. (2005). Surgical resection of primary tumors in patients who present with stage IV colorectal cancer: An analysis of surveillance, epidemiology, and end results data, 1988 to 2000. *Annals of Surgical Oncology*, *12*(8), 637–645. https://doi.org/10.1245/ASO.2005.06.012

Corbet, C., & Feron, O. (2017, October 1). Tumour acidosis: From the passenger to the driver's seat. *Nature Reviews Cancer*. Nature Publishing Group. https://doi.org/10.1038/nrc.2017.77

Cowley, G. S., Weir, B. A., Vazquez, F., Tamayo, P., Scott, J. A., Rusin, S., … Hahn, W. C. (2014). Parallel genome-scale loss of function screens in 216 cancer cell lines for the identification of context-specific genetic dependencies. *Scientific Data*, *1*. https://doi.org/10.1038/sdata.2014.35

Daenen, L. G. M., Roodhart, J. M. L., Van Amersfoort, M., Dehnad, M., Roessingh, W., Ulfman, L. H., … Voest, E. E. (2011). Chemotherapy enhances metastasis formation via VEGFR-1-expressing endothelial cells. *Cancer Research*, *71*(22), 6976–6985. https://doi.org/10.1158/0008-5472.CAN-11-0627

Demirkol Canll, S., Seza, E. G., Sheraj, I., Gömçeli, I., Turhan, N., Carberry, S., … Banerjee, S. (2020). Evaluation of an aldo-keto reductase gene signature with prognostic significance in colon cancer via activation of epithelial to mesenchymal transition and the p70S6K pathway. *Carcinogenesis*, *41*(9), 1219–1228. https://doi.org/10.1093/carcin/bgaa072

Desch, C. E., Benson, A. B., Somerfield, M. R., Flynn, P. J., Krause, C., Loprinzi, C. L., … Petrelli, N. J. (2005). Colorectal cancer surveillance: 2005 Update of an American Society of Clinical Oncology practice guideline. *Journal of Clinical Oncology*, *23*(33), 8512–8519. https://doi.org/10.1200/JCO.2005.04.0063

Díaz, F. E., Dantas, E., & Geffner, J. (2018). Unravelling the Interplay between Extracellular Acidosis and Immune Cells. *Mediators of Inflammation*, *2018*. https://doi.org/10.1155/2018/1218297

DiStefano, J., & Davis, B. (2019). Diagnostic and Prognostic Potential of AKR1B10 in Human Hepatocellular Carcinoma. *Cancers*, *11*(4), 486. https://doi.org/10.3390/cancers11040486

Dvornik, D., Simard-Duquesne, N., Krami, M., Sestanj, K., Gabbay, K. H., Kinoshita, J. H., … Merola, L. O. (1973). Polyol accumulation in galactosemic and diabetic rats: Control by an aldose reductase inhibitor. *Science*, *182*(4117), 1146–1148. https://doi.org/10.1126/science.182.4117.1146

Ehrig, T., Prendergast, F. G., Bohren, K. M., Gabbay, K. H., & Gabbay, K. H. (1994). Mechanism of Aldose Reductase Inhibition: Binding of NADP+/NADPH and Alrestatin-like Inhibitors. *Biochemistry*, *33*(23), 7157–7165. https://doi.org/10.1021/bi00189a019

Ellis, E. M. (2002). Microbial aldo-keto reductases. *FEMS Microbiology Letters*, *216*(2), 123–131. https://doi.org/10.1111/j.1574-6968.2002.tb11425.x

Fan, J., Ye, J., Kamphorst, J. J., Shlomi, T., Thompson, C. B., & Rabinowitz, J. D. (2014). Quantitative flux analysis reveals folate-dependent NADPH production. *Nature*, *510*(7504), 298–302. https://doi.org/10.1038/nature13236

Feoktistova, M., Geserick, P., & Leverkus, M. (2016). Crystal violet assay for determining viability of cultured cells. *Cold Spring Harbor Protocols*, *2016*(4), 343–346. https://doi.org/10.1101/pdb.prot087379

Fukumoto, S. I., Yamauchi, N., Moriguchi, H., Hippo, Y., Watanabe, A., Shibahara, J., … Aburatani, H. (2005). Overexpression of the aldo-keto reductase family protein AKR1B10 is highly correlated with smokers' non-small cell lung carcinomas. *Clinical Cancer Research*, *11*(5), 1776–1785. https://doi.org/10.1158/1078-0432.CCR-04-1238

Gabbay, K. H. (2004). Aldose reductase inhibition in the treatment of diabetic neuropathy: Where are we in 2004? *Current Diabetes Reports*. Current Science Ltd. https://doi.org/10.1007/s11892-004-0047-z

Gabbay, K. H., Merola, L. O., & Field, R. A. (1966). Sorbitol pathway: Presence in nerve and cord with substrate accumulation in diabetes. *Science*, *151*(3707), 209–210. https://doi.org/10.1126/science.151.3707.209

Gallego, O., Belyaeva, O. V., Porté, S., Ruiz, F. X., Stetsenko, A. V., Shabrova, E. V., … Kedishvili, N. Y. (2006). Comparative functional analysis of human medium-chain dehydrogenases, short-chain dehydrogenases/reductases and aldo-keto reductases with retinoids. *Biochemical Journal*, *399*(1), 101–109. https://doi.org/10.1042/BJ20051988

Gallego, O., Ruiz, F. X., Ardèvol, A., Domínguez, M., Alvarez, R., De Lera, A. R., … Parés, X. (2007). Structural basis for the high all-trans-retinaldehyde reductase activity of the tumor marker AKR1B10. *Proceedings of the*

National Academy of Sciences of the United States of America, *104*(52), 20764–20769. https://doi.org/10.1073/pnas.0705659105

Gauthier, L. D., Greenstein, J. L., O'Rourke, B., & Winslow, R. L. (2013). An integrated mitochondrial ROS production and scavenging model: Implications for heart failure. *Biophysical Journal*, *105*(12), 2832–2842. https://doi.org/10.1016/j.bpj.2013.11.007

Ge, T., Yang, J., Zhou, S., Wang, Y., Li, Y., & Tong, X. (2020, June 9). The Role of the Pentose Phosphate Pathway in Diabetes and Cancer. *Frontiers in Endocrinology*. Frontiers Media S.A. https://doi.org/10.3389/fendo.2020.00365

Hanahan, D., & Weinberg, R. A. (2011, March 4). Hallmarks of cancer: The next generation. *Cell*. Elsevier. https://doi.org/10.1016/j.cell.2011.02.013

Heiden, M. G. V., Cantley, L. C., & Thompson, C. B. (2009, May 22). Understanding the warburg effect: The metabolic requirements of cell proliferation. *Science*. NIH Public Access. https://doi.org/10.1126/science.1160809

Hu, Y. Y., Zheng, M. H., Zhang, R., Liang, Y. M., & Han, H. (2012). Notch signaling pathway and cancer metastasis. *Advances in Experimental Medicine and Biology*, *727*, 186–198. https://doi.org/10.1007/978-1-4614-0899-4_14

Huang, C., Sheng, S., Li, R., Sun, X., Liu, J., & Huang, G. (2015). Lactate promotes resistance to glucose starvation via upregulation of Bcl-2 mediated by mTOR activation. *Oncology Reports*, *33*(2), 875–884. https://doi.org/10.3892/or.2014.3655

Hyndman, D. J., & Flynn, T. G. (1998). Sequence and expression levels in human tissues of a new member of the aldo-keto reductase family. *Biochimica et Biophysica Acta - Gene Structure and Expression*, *1399*(2–3), 198–202. https://doi.org/10.1016/S0167-4781(98)00109-2

Jang, S. H., Kim, A. R., Park, N. H., Park, J. W., & Han, I. S. (2016). DRG2 regulates G2/M progression via the cyclin B1-Cdk1 complex. *Molecules and Cells*, *39*(9), 699–704. https://doi.org/10.14348/molcells.2016.0149

Jez, J. M., Bennett, M. J., Schlegel, B. P., Lewis, M., & Penning, T. M. (1997). Comparative anatomy of the aldo–keto reductase superfamily. *Biochemical Journal*, *326*(3), 625–636. https://doi.org/10.1042/BJ3260625

Jiang, P., Du, W., Wang, X., Mancuso, A., Gao, X., Wu, M., & Yang, X. (2011). P53 regulates biosynthesis through direct inactivation of glucose-6-phosphate

dehydrogenase. *Nature Cell Biology*, *13*(3), 310–316. https://doi.org/10.1038/ncb2172

Ju, H. Q., Lin, J. F., Tian, T., Xie, D., & Xu, R. H. (2020, December 1). NADPH homeostasis in cancer: functions, mechanisms and therapeutic implications. *Signal Transduction and Targeted Therapy*. Springer Nature. https://doi.org/10.1038/s41392-020-00326-0

Kaiserova, K., Tang, X. L., Srivastava, S., & Bhatnagar, A. (2008). Role of nitric oxide in regulating aldose reductase activation in the ischemic heart. *Journal of Biological Chemistry*, *283*(14), 9101–9112. https://doi.org/10.1074/jbc.M709671200

Kuehne, A., Emmert, H., Soehle, J., Winnefeld, M., Fischer, F., Wenck, H., … Zamboni, N. (2015). Acute Activation of Oxidative Pentose Phosphate Pathway as First-Line Response to Oxidative Stress in Human Skin Cells. *Molecular Cell*, *59*(3), 359–371. https://doi.org/10.1016/j.molcel.2015.06.017

Lee, S. B., Kim, J. J., Kim, T. W., Kim, B. S., Lee, M. S., & Yoo, Y. Do. (2010). Serum deprivation-induced reactive oxygen species production is mediated by Romo1. *Apoptosis*, *15*(2), 204–218. https://doi.org/10.1007/s10495-009-0411-1

Lee, Y. J., Shin, K. J., Park, S. A., Park, K. S., Park, S., Heo, K., … Suh, P. G. (2016). G-protein-coupled receptor 81 promotes a malignant phenotype in breast cancer through angiogenic factor secretion. *Oncotarget*, *7*(43), 70898–70911. https://doi.org/10.18632/oncotarget.12286

Levin, R. J. (1994). Digestion and absorption of carbohydrates - From molecules and membranes to humans. In *American Journal of Clinical Nutrition* (Vol. 59). American Society for Nutrition. https://doi.org/10.1093/ajcn/59.3.690S

Ling, Y. H., Consoli, U., Tornos, C., Andreeff, M., & Perez-Soler, R. (1998). Accumulation of cyclin B1, activation of cyclin B1-dependent kinase and induction of programmed cell death in human epidermoid carcinoma KB cells treated with taxol. *International Journal of Cancer,* 75(6), 925–932. https://doi.org/10.1002/(SICI)1097-0215(19980316)75:6<925::AID-IJC16>3.0.CO;2-1

Locasale, J. W. (2013, August). Serine, glycine and one-carbon units: Cancer metabolism in full circle. *Nature Reviews Cancer*. Nat Rev Cancer. https://doi.org/10.1038/nrc3557

Lunt, S. Y., & Vander Heiden, M. G. (2011). Aerobic glycolysis: meeting the metabolic requirements of cell proliferation. *Annual Review of Cell and*

Developmental Biology, *27*(1), 441–464. https://doi.org/10.1146/annurev-cellbio-092910-154237

Ma, J., Yan, R., Zu, X., Cheng, J. M., Rao, K., Liao, D. F., & Cao, D. (2008). Aldo-keto reductase family 1 B10 affects fatty acid synthesis by regulating the stability of acetyl-CoA carboxylase-α in breast cancer cells. *Journal of Biological Chemistry*, *283*(6), 3418–3423. https://doi.org/10.1074/jbc.M707650200

Martin, H. J., Breyer-Pfaff, U., Wsol, V., Venz, S., Block, S., & Maser, E. (2006). Purification and characterization of AKR1B10 from human liver: Role in carbonyl reduction of xenobiotics. *Drug Metabolism and Disposition*, *34*(3), 464–470. https://doi.org/10.1124/dmd.105.007971

Mookerjee, S. A., Gerencser, A. A., Nicholls, D. G., & Brand, M. D. (2017). Quantifying intracellular rates of glycolytic and oxidative ATP production and consumption using extracellular flux measurements. *Journal of Biological Chemistry*, *292*(17), 7189–7207. https://doi.org/10.1074/jbc.M116.774471

Mueckler, M., & Thorens, B. (2013, April). The SLC2 (GLUT) family of membrane transporters. *Molecular Aspects of Medicine*. NIH Public Access. https://doi.org/10.1016/j.mam.2012.07.001

Nakazawa, M. S., Keith, B., & Simon, M. C. (2016, September 23). Oxygen availability and metabolic adaptations. *Nature Reviews Cancer*. Nature Publishing Group. https://doi.org/10.1038/nrc.2016.84

Nicolucci, A., Carinci, F., Cavaliere, D., Scorpiglione, N., Belfiglio, M., Labbrozzi, D., … Liberati, A. (1996). A meta-analysis of trials on aldose reductase inhibitors in diabetic peripheral neuropathy. *Diabetic Medicine*, *13*(12), 1017–1026. https://doi.org/10.1002/(SICI)1096-9136(199612)13:12<1017::AID-DIA252>3.0.CO;2-Z

Nishinaka, T., Azuma, Y., Ushijima, S., Miki, T., & Yabe-Nishimura, C. (2003). Human testis specific protein: A new member of aldo-keto reductase superfamily. In *Chemico-Biological Interactions* (Vol. 143–144, pp. 299–305). Chem Biol Interact. https://doi.org/10.1016/S0009-2797(02)00187-4

Ohashi, T., Idogawa, M., Sasaki, Y., Suzuki, H., & Tokino, T. (2013). AKR1B10, a transcriptional target of p53, is downregulated in colorectal cancers associated with poor prognosis. *Molecular Cancer Research*, *11*(12), 1554–1563. https://doi.org/10.1158/1541-7786.MCR-13-0330-T

Patra, K. C., & Hay, N. (2014). The pentose phosphate pathway and cancer. *Trends in Biochemical Sciences*. Elsevier Ltd. https://doi.org/10.1016/j.tibs.2014.06.005

Pavlova, N. N., & Thompson, C. B. (2016, January 12). The Emerging Hallmarks of Cancer Metabolism. *Cell Metabolism*. Cell Press. https://doi.org/10.1016/j.cmet.2015.12.006

Penning, T. M., & Byrns, M. C. (2009). Steroid hormone transforming aldo-keto reductases and cancer. In *Annals of the New York Academy of Sciences* (Vol. 1155, pp. 33–42). Blackwell Publishing Inc. https://doi.org/10.1111/j.1749-6632.2009.03700.x

Petrashsjli, J. M., Harters, T. M., Devine11, C. S., Olinslj, P. 0, Bhatnagar, A., Liu, S., & Srivastava, S. K. (1992). Involvement of Cysteine Residues in Catalysis and Inhibition of Human Aldose Reductase :SITE-DIRECTED MUTAGENESIS OF CYS-80,-298, AND-303* *The Journal of Biological Chemistry* (Vol. 267).

Pfaffl, M. W. (2001). A new mathematical model for relative quantification in real-time RT-PCR. *Nucleic Acids Research*, *29*(9), e45. https://doi.org/10.1093/nar/29.9.e45

Pfeiffer, T., Schuster, S., & Bonhoeffer, S. (2001). Cooperation and competition in the evolution of ATP-producing pathways. *Science*, *292*(5516), 504–507. https://doi.org/10.1126/science.1058079

Pollak, N., Dölle, C., & Ziegler, M. (2007, March 1). The power to reduce: Pyridine nucleotides - Small molecules with a multitude of functions. *Biochemical Journal*. Biochem J. https://doi.org/10.1042/BJ20061638

Pretzsch, E., Bösch, F., Neumann, J., Ganschow, P., Bazhin, A., Guba, M., … Angele, M. (2019). Mechanisms of Metastasis in Colorectal Cancer and Metastatic Organotropism: Hematogenous versus Peritoneal Spread. https://doi.org/10.1155/2019/7407190

Ramana, K. V. (2011, April 1). Aldose reductase: New insights for an old enzyme. *Biomolecular Concepts*. Walter de Gruyter GmbH. https://doi.org/10.1515/bmc.2011.002

Ramana, K. V., Chandra, D., Srivastava, S., Bhatnagar, A., & Srivastava, S. K. (2003). Nitric oxide regulates the polyol pathway of glucose metabolism in vascular smooth muscle cells. *The FASEB Journal*, *17*(3), 417–425. https://doi.org/10.1096/fj.02-0722com

Ramana, K. V., Chandra, D., Srivastava, S., Bhatnagar, A., & Srivastava, S. K. (2003). Aldose reductase mediates the mitogenic signals of cytokines. In *Chemico-Biological Interactions* (Vol. 143–144, pp. 587–596). Chem Biol Interact. https://doi.org/10.1016/S0009-2797(02)00194-1

Ramana, K. V., Fadl, A. A., Tammali, R., Reddy, A. B. M., Chopra, A. K., & Srivastava, S. K. (2006). Aldose reductase mediates the lipopolysaccharide-induced release of inflammatory mediators in RAW264.7 murine macrophages. *Journal of Biological Chemistry*, *281*(44), 33019–33029. https://doi.org/10.1074/jbc.M603819200

Ramana, K. V., Friedrich, B., Tammali, R., West, M. B., Bhatnagar, A., & Srivastava, S. K. (2005). Requirement of aldose reductase for the hyperglycemic activation of protein kinase C and formation of diacylglycerol in vascular smooth muscle cells. *Diabetes*, *54*(3), 818–829. https://doi.org/10.2337/diabetes.54.3.818

Ramana, K. V., Tammali, R., Reddy, A. B. M., Bhatnagar, A., & Srivastava, S. K. (2007). Aldose reductase-regulated tumor necrosis factor-α production is essential for high glucose-induced vascular smooth muscle cell growth. *Endocrinology*, *148*(9), 4371–4384. https://doi.org/10.1210/en.2007-0512

Ray, P. D., Huang, B. W., & Tsuji, Y. (2012, May). Reactive oxygen species (ROS) homeostasis and redox regulation in cellular signaling. *Cellular Signalling*. Cell Signal. https://doi.org/10.1016/j.cellsig.2012.01.008

Rhee, E. J., & Plutzky, J. (2012, June). Retinoid metabolism and diabetes mellitus. *Diabetes and Metabolism Journal*. Korean Diabetes Association. https://doi.org/10.4093/dmj.2012.36.3.167

Riganti, C., Gazzano, E., Polimeni, M., Aldieri, E., & Ghigo, D. (2012, August 1). The pentose phosphate pathway: An antioxidant defense and a crossroad in tumor cell fate. *Free Radical Biology and Medicine*. Pergamon. https://doi.org/10.1016/j.freeradbiomed.2012.05.006

Ruiz, F. X., Porté, S., Parés, X., & Farrés, J. (2012). Biological role of aldo-keto reductases in retinoic acid biosynthesis and signaling. *Frontiers in Pharmacology*, *3 APR*. https://doi.org/10.3389/fphar.2012.00058

Schwab, A., Siddiqui, A., Vazakidou, M. E., Napoli, F., Bottcher, M., Menchicchi, B., … Ceppi, P. (2018). Polyol pathway links glucose metabolism to the aggressiveness of cancer cells. *Cancer Research*, *78*(7), 1604–1618. https://doi.org/10.1158/0008-5472.CAN-17-2834

Seyfried, T. N., & Huysentruyt, L. C. (2013). On the origin of cancer metastasis. *Critical Reviews in Oncogenesis*, *18*(1–2), 43–73. https://doi.org/10.1615/CritRevOncog.v18.i1-2.40

Shestov, A. A., Liu, X., Ser, Z., Cluntun, A. A., Hung, Y. P., Huang, L., … Locasale, J. W. (2014). Quantitative determinants of aerobic glycolysis identify flux through the enzyme GAPDH as a limiting step. *ELife*, *3*(July2014), 1–18. https://doi.org/10.7554/eLife.03342

Shiratori, R., Furuichi, K., Yamaguchi, M., Miyazaki, N., Aoki, H., Chibana, H., … Aoki, S. (2019). Glycolytic suppression dramatically changes the intracellular metabolic profile of multiple cancer cell lines in a mitochondrial metabolism-dependent manner. *Scientific Reports*, *9*(1), 1–15. https://doi.org/10.1038/s41598-019-55296-3

Simpson, T., Pase, M., & Stough, C. (2015). Bacopa monnieri as an Antioxidant Therapy to Reduce Oxidative Stress in the Aging Brain. *Evidence-Based Complementary and Alternative Medicine*. Hindawi Limited. https://doi.org/10.1155/2015/615384

Sugita, S., Kamei, Y., Akaike, F., Suganami, T., Kanai, S., Hattori, M., … Ogawa, Y. (2011). Increased systemic glucose tolerance with increased muscle glucose uptake in transgenic mice overexpressing RXRγ in skeletal muscle. *PLoS ONE*, *6*(5). https://doi.org/10.1371/journal.pone.0020467

Tang, M., Etokidem, E., & Lai, K. (2016). The leloir pathway of galactose metabolism - A novel therapeutic target for hepatocellular carcinoma. *Anticancer Research*, *36*(12), 6265–6271. https://doi.org/10.21873/anticanres.11221

Tang, W. H., Martin, K. A., & Hwa, J. (2012). Aldose reductase, oxidative stress, and diabetic mellitus. *Frontiers in Pharmacology*, *3 MAY*. https://doi.org/10.3389/fphar.2012.00087

Tang, X., Kuhlenschmidt, T. B., Li, Q., Ali, S., Lezmi, S., Chen, H., … Kuhlenschmidt, M. S. (2014). A mechanically-induced colon cancer cell population shows increased metastatic potential. *Molecular Cancer*, *13*(1), 131. https://doi.org/10.1186/1476-4598-13-131

Taskoparan, B., Seza, E. G., Demirkol, S., Tuncer, S., Stefek, M., Gure, A. O., & Banerjee, S. (2017). Opposing roles of the aldo-keto reductases AKR1B1 and AKR1B10 in colorectal cancer. *Cellular Oncology*, *40*(6), 563–578. https://doi.org/10.1007/s13402-017-0351-7

Van Roy, F. (2014, February 20). Beyond E-cadherin: Roles of other cadherin superfamily members in cancer. *Nature Reviews Cancer*. Nature Publishing Group. https://doi.org/10.1038/nrc3647

van Weverwijk, A., Koundouros, N., Iravani, M., Ashenden, M., Gao, Q., Poulogiannis, G., … Isacke, C. M. (2019). Metabolic adaptability in metastatic breast cancer by AKR1B10-dependent balancing of glycolysis and fatty acid oxidation. *Nature Communications*, *10*(1), 1–13. https://doi.org/10.1038/s41467-019-10592-4

Wallner, E. I., Wada, J., Tramonti, G., Lin, S., Srivastava, S. K., & Kanwar, Y. S. (2001). Relevance of aldo-keto reductase family members to the pathobiology of diabetic nephropathy and renal development. In *Renal Failure* (Vol. 23, pp. 311–320). Ren Fail. https://doi.org/10.1081/JDI-100104715

Wang, Y. Y., Qi, L. N., Zhong, J. H., Qin, H. G., Ye, J. Z., Lu, S. D., … You, X. M. (2017). High expression of AKR1B10 predicts low risk of early tumor recurrence in patients with hepatitis B virus-related hepatocellular carcinoma. *Scientific Reports*, *7*(1), 1–9. https://doi.org/10.1038/srep42199

Wang, Y., Xia, Y., & Lu, Z. (2018). Metabolic features of cancer cells 06 Biological Sciences 0601 Biochemistry and Cell Biology. *Cancer Communications*, *38*(1). https://doi.org/10.1186/s40880-018-0335-7

Weber, S., Salabei, J. K., Möller, G., Kremmer, E., Bhatnagar, A., Adamski, J., & Barski, O. A. (2015). Aldo-keto Reductase 1B15 (AKR1B15): A mitochondrial human aldo-keto reductase with activity toward steroids and 3-keto-acyl-CoA conjugates. *Journal of Biological Chemistry*, *290*(10), 6531–6545. https://doi.org/10.1074/jbc.M114.610121

Wells, A., Grahovac, J., Wheeler, S., Ma, B., & Lauffenburger, D. (2013, May). Targeting tumor cell motility as a strategy against invasion and metastasis. *Trends in Pharmacological Sciences*. https://doi.org/10.1016/j.tips.2013.03.001

Whiteside, T. L. (2008, October 6). The tumor microenvironment and its role in promoting tumor growth. *Oncogene*. NIH Public Access. https://doi.org/10.1038/onc.2008.271

Wongtangtintharn, S., Oku, H., Iwasaki, H., & Toda, T. (2004). Effect of branched-chain fatty acids on fatty acid biosynthesis of human breast cancer cells. *Journal of Nutritional Science and Vitaminology*, *50*(2), 137–143. https://doi.org/10.3177/jnsv.50.137

Wu, X., Li, X., Fu, Q., Cao, Q., Chen, X., Wang, M., … Dong, C. (2017). AKR1B1 promotes basal-like breast cancer progression by a positive feedback loop that activates the EMT program. *Journal of Experimental Medicine*, *214*(4), 1065–1079. https://doi.org/10.1084/jem.20160903

Xu, K., Yin, N., Peng, M., Stamatiades, E. G., Shyu, A., Li, P., … Li, M. O. (2021). Glycolysis fuels phosphoinositide 3-kinase signaling to bolster T cell immunity. *Science*, *371*(6527), 405–410. https://doi.org/10.1126/science.abb2683

Yan, R., Zu, X., Ma, J., Liu, Z., Adeyanju, M., & Cao, D. (2007). Aldo-keto reductase family 1 B10 gene silencing results in growth inhibition of colorectal cancer cells: Implication for cancer intervention. *International Journal of Cancer*, *121*(10), 2301–2306. https://doi.org/10.1002/ijc.22933

Yao, Y., Wang, X., Zhou, D., Li, H., Qian, H., Zhang, J., … Zhu, X. (2020). Loss of AKR1B10 promotes colorectal cancer cells proliferation and migration via regulating FGF1-dependent pathway. *Aging*, *12*(13), 13059–13075. https://doi.org/10.18632/aging.103393

Yang, W., & Lu, Z. (2015). Pyruvate kinase M2 at a glance. *Journal of Cell Science*, *128*(9), 1655–1660. https://doi.org/10.1242/jcs.166629

Yoshitake, H., Takahashi, M., Ishikawa, H., Nojima, M., Iwanari, H., Watanabe, A., … Araki, Y. (2007). Aldo-keto reductase family 1, member B10 in uterine carcinomas: A potential risk factor of recurrence after surgical therapy in cervical cancer. *International Journal of Gynecological Cancer*, *17*(6), 1300–1306. https://doi.org/10.1111/j.1525-1438.2007.00932.x

APPENDICES

A. Plasmids used for Lentivirus Generation

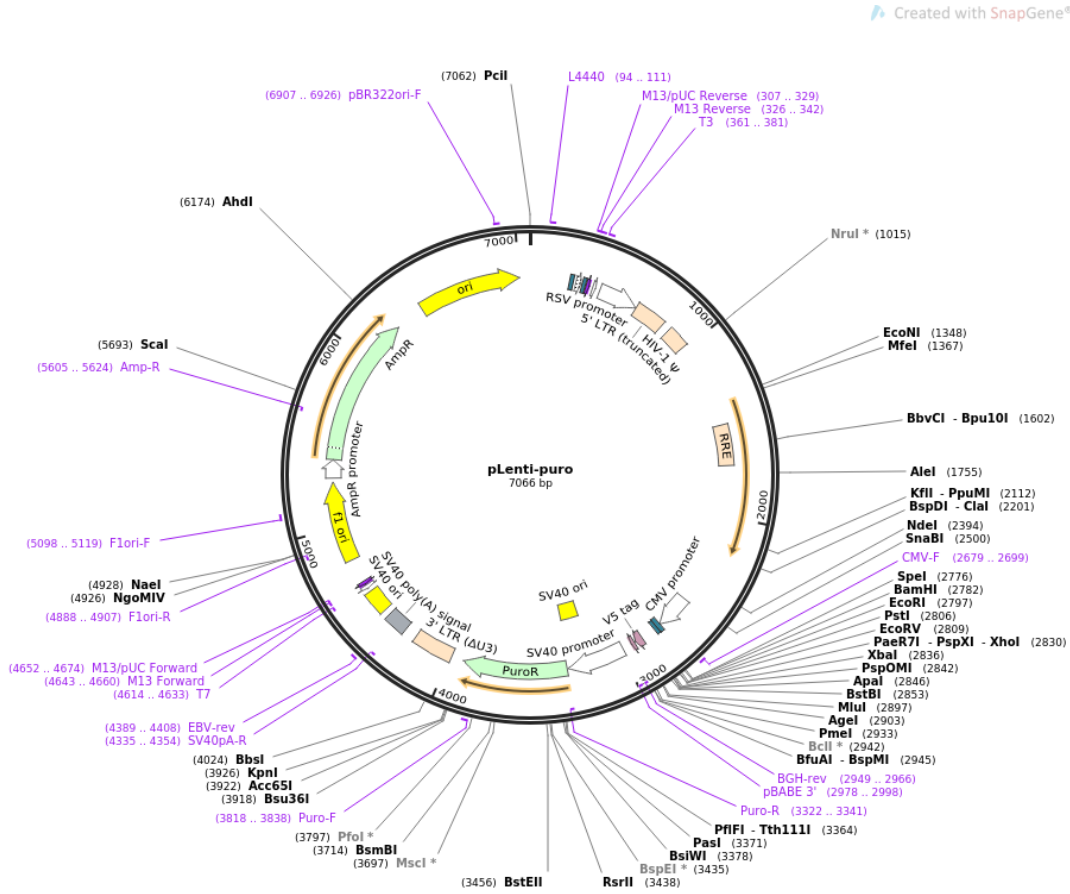

Supp. Figure 1. *Vector map of Tetracycline inducible 3rd generation lentiviral vector pLenti-puro*

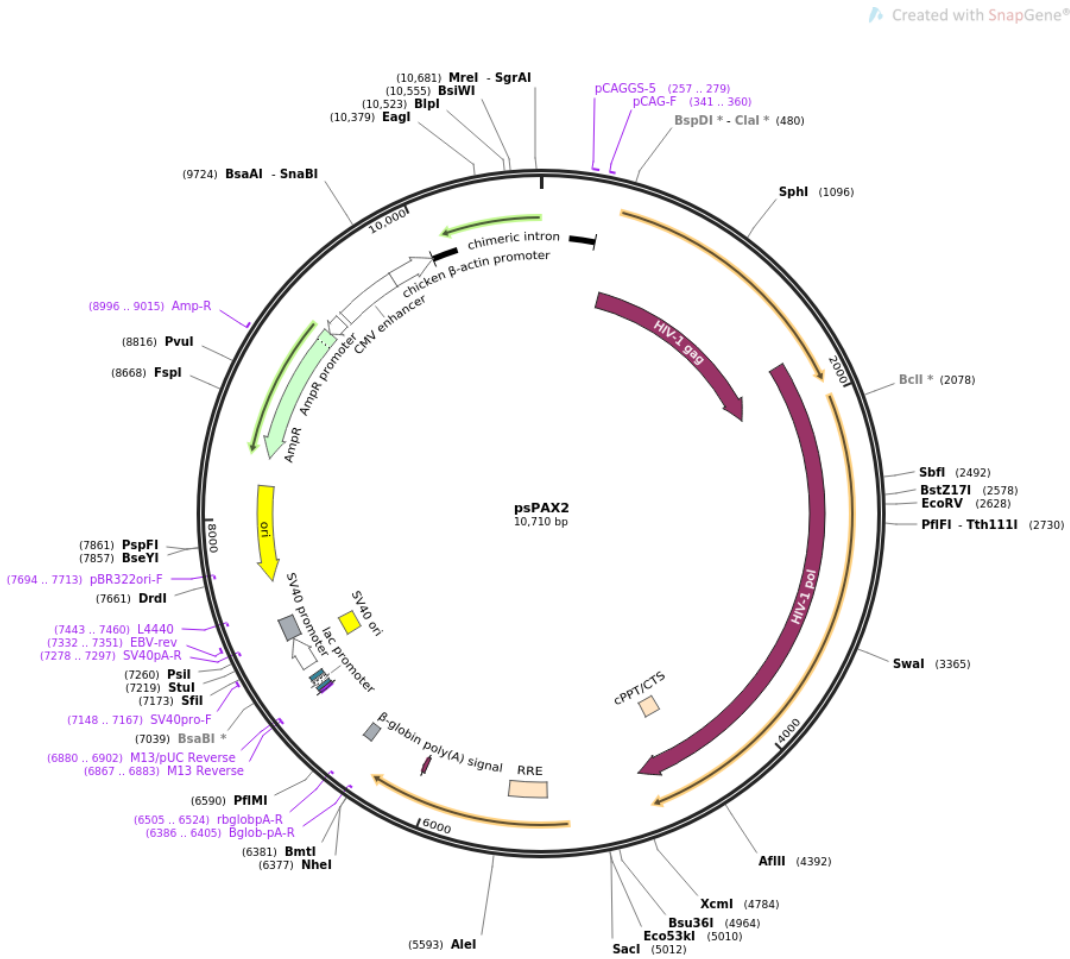

Supp. Figure 2. *Vector map of 2nd generation lentiviral packaging plasmid psPAX2*

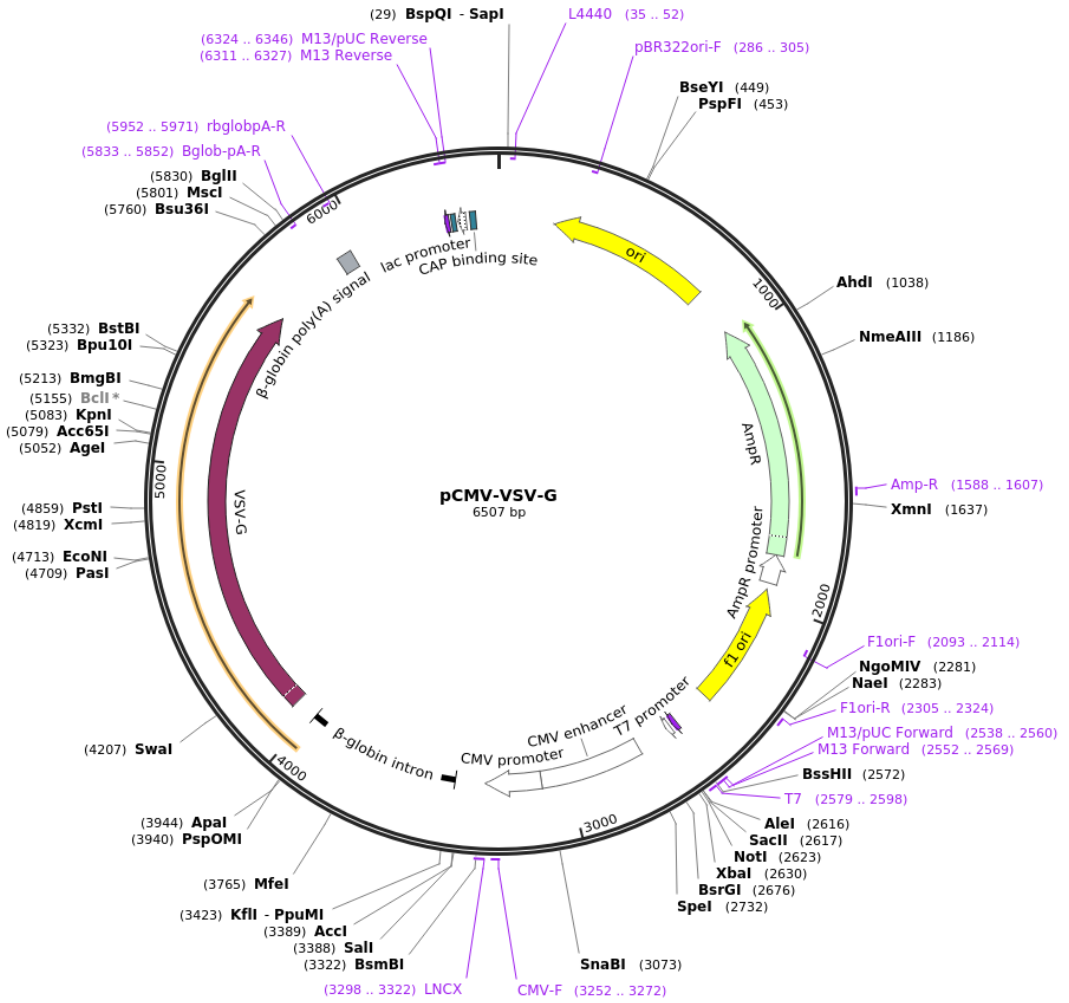

Supp. Figure 3. *Vector map of pCMV-VSV-G, envelope protein for producing lentiviral and MuLV retroviral particles*

B. Contents of Buffers Used in Western Blotting

Table 4. *Western blotting buffer contents*

6x Sample Loading Dye	10x Blotting Buffer	Transfer Buffer (for 1L)	SDS-PAGE Running Buffer	10% Separating Gel Mix	4% Separating Gel Mix	TBS-T	Mild Stripping Buffer
12% SDS	0.25 M Tris	200 mL Methanol	25 mM Tris	5.4 mL dH_2O	4.7 mL dH_2O	50 mM Tris-HCl at pH 7.4	15 g Glycine
30% β-mercaptoethanol	1.92 M Glycine	100 mL 10x Blotting Buffer	190 mM Glycine	3.8 mL 10% SDS + 1.5 M Tris-HCl at pH 8.8	2 mL 10% SDS + 1.5 M Tris-HCl at pH 6.8	150 mM NaCl	1 g SDS
30% Glycerol	Adjusted pH to 8.3 in 1L dH_2O		0.1% SDS	5.6 mL 30% Acrylamide-Bisacrylamide Solution	1.2 mL 30% Acrylamide-Bisacrylamide Solution	Autoclaved for sterility and 0.1% Tween-20 added before using	10 mL Tween-20
0.012% Bromophenol Blue		700 mL dH_2O		150 µL 10% Ammonium persulfate	50 µL 10% Ammonium persulfate		Adjusted to pH 2.2 in 1L of dH2O
0.375 M Tris-HCl pH 6.8				20 µL TEMED	10 µL TEMED		